forests

MDPI

Article

Vegetation Structure, Surface-Active Brachyuran Assemblages, and Selected Environmental Conditions in a Replanted *Rhizophora mucronata* Mangrove Stand

Arida Fauziyah [1,2,3], Angga Dwiartama [1], Marc Kochzius [2], Risma Illa Maulany [3] and Intan Ahmad [1,*]

[1] School of Life Sciences and Technology, Institut Teknologi Bandung (ITB), Bandung 40132, Indonesia; fauziyaharida@gmail.com (A.F.); dwiartama@itb.ac.id (A.D.)
[2] Marine Biology, Vrije Universiteit Brussel (VUB), 1050 Brussels, Belgium; marc.kochzius@vub.be
[3] Faculty of Forestry, Hasanuddin University (Unhas), Makassar 90245, Indonesia; risma.maulany@unhas.ac.id
* Correspondence: intan@itb.ac.id

Abstract

Mangrove replantation is widely implemented as a rehabilitation-oriented response to coastal degradation, yet many replanted stands remain poorly assessed after plantation. This study provides a preliminary dry-season post-plantation habitat characterization of an eight-year-old replanted *Rhizophora mucronata* stand at Sungai Ujung River, South Sulawesi, Indonesia. Its novelty lies in integrating vegetation structure, surface-active brachyuran taxonomic units, selected surface-water variables, and sediment texture within a single replanted stand where no baseline or long-term monitoring data were available. The final descriptive dataset included seven plots across three transects. Surface-active brachyurans and water-quality variables were recorded across five valid sampling occasions: three spring-tide and two neap-tide occasions. Because tidal period was a sampling-occasion-level condition and temporal replication was limited, spring–neap patterns were interpreted descriptively. Eight surface-active brachyuran taxonomic units comprising 676 individuals were recorded, dominated by *Metopograpsus latifrons*. Crab abundance, Shannon diversity, and water-quality profiles varied among occasions and plots. All 113 living mangrove individuals were *R. mucronata*, with established trees, visible seedlings, and scarce poles. Sediment texture ranged from sand-dominated to clay-rich substrates. These findings provide a structured reference point for future monitoring, but do not demonstrate replantation success, recovery trajectory, or functional recovery.

Keywords: post-plantation assessment; habitat characterization; replantation monitoring; intertidal crabs; mangrove stand structure

Check for updates

Academic Editor: Daniel M. Alongi

Received: 18 July 2026
Revised: 23 August 2026
Accepted: 25 August 2026
Published: 4 September 2026

Copyright: © 2026 by the authors. Licensee MDPI, Basel, Switzerland. This article is an open access article distributed under the terms and conditions of the Creative Commons Attribution (CC BY) license.

1. Introduction

Mangrove ecosystems provide essential ecological functions, including coastal protection, carbon storage, nutrient cycling, sediment stabilization, and habitat provision for diverse terrestrial, estuarine, and marine fauna [1–4]. Despite these ecological and socioeconomic roles, mangrove ecosystems continue to be degraded throughout the Indo-Pacific region, including Indonesia, where aquaculture development has been one of the major drivers of mangrove conversion [5–8]. In response to such degradation, mangrove replantation has been widely implemented as a rehabilitation-oriented intervention. However, many replantation efforts remain poorly documented after planting, resulting in limited

understanding of stand development, faunal recolonization, environmental condition, and longer-term habitat change [9,10].

Post-plantation assessment is essential because plantation alone does not demonstrate ecological recovery or functional rehabilitation. Bosire et al. [5] emphasized that many mangrove replantation efforts have occurred without sufficient assessment of ecosystem-level recovery and argued that ecosystem-level monitoring should be an integral component of replantation projects. Their restoration framework recommends assessment of success and functionality through several broad components, including vegetation development and floristic succession, faunistic recruitment, environmental factors and processes, and potential sustainable utilization [11]. Such assessment is particularly important in replanted mangrove areas where original baselines are absent, planting histories are incompletely documented, and management decisions are often made without structured ecological information.

In this study, habitat characterization was based on four selected components: vegetation structure, surface-active brachyuran taxonomic units, and selected water-quality variables. Vegetation structure was included because it directly describes the present condition of the replanted mangrove stand, including the establishment of tree-stage individuals, the presence of seedlings, the representation of intermediate pole-stage individuals, stand density, and basal area [12]. These variables provide a practical description of stand structure and regeneration potential, although they do not by themselves demonstrate recovery trajectory or replantation success. Surface-active brachyuran crabs were included as a practical faunal descriptor of the visible mangrove-floor assemblage during low tide. Brachyuran crabs are widely recognized as ecologically important mangrove-associated fauna because many taxa contribute to litter processing, trophic transfer, sediment modification, propagule predation, and nutrient cycling [13–16]. However, the present study focused only on intact, visible, surface-active individuals encountered during low-tide sampling. This approach was chosen because it provides a standardized and feasible snapshot of detectable mangrove-floor fauna, but it does not represent the full intertidal crab community. Surface-active or non-burrowing brachyurans may use root crevices, shallow sediment burying, existing burrows, or other behavioral strategies to persist in intertidal habitats [13–15,17,18]. Therefore, the crab data were interpreted as surface-active brachyuran taxonomic units rather than as comprehensive crab diversity or direct evidence of functional recovery. Selected water-quality variables, namely salinity, pH, and total dissolved solids (TDS), were measured to provide basic physicochemical context for the replanted mangrove habitat [19,20]. Salinity is a central descriptor of estuarine and mangrove water conditions because it reflects the balance between marine influence, freshwater input, evaporation, and tidal exchange. pH provides a general indicator of water acidity or alkalinity, while TDS describes the concentration of dissolved ions and solids in the water column.

Sungai Ujung River in Maros, South Sulawesi, Indonesia, contains a mangrove area replanted with *Rhizophora mucronata* Poir. in 2015 based on local information. However, no pre-plantation baseline, early post-plantation assessment, or continuous monitoring record is available for this site. Consequently, the development trajectory and present habitat condition of the replanted stand remain poorly documented. This situation reflects a common challenge in mangrove replantation programs, where planting activities are implemented but subsequent ecological assessment is limited [5,21].

Because no baseline or temporal monitoring data were available for the Sungai Ujung replantation site, this study does not evaluate replantation trajectory, rehabilitation success, or functional recovery. Instead, it provides a preliminary dry-season post-plantation characterization of selected habitat attributes approximately eight years after plantation.

Specifically, this study addressed three questions: (1) What surface-active brachyuran taxonomic units were recorded in the replanted *R. mucronata* stand, and how were their abundance and diversity distributed across plots and sampling occasions? (2) How did selected plot-level surface-water variables vary descriptively across sampling occasions? (3) What vegetation structure and sediment texture characterized the replanted mangrove stand across transects? By documenting vegetation structure, surface-active brachyuran taxonomic units, selected water-quality variables, and sediment texture, this study provides a structured reference point for future monitoring of the Sungai Ujung replanted mangrove stand.

2. Materials and Methods

This study was conducted at the mangrove-fringed brackish water river Sungai Ujung, located in the western Maros Regency, South Sulawesi Province, Indonesia (Figure 1a–d). Sampling was conducted twice monthly from June to September 2023, during both spring and neap tides. Three transects were established, each consisting of a maximum of three plots arranged along a 30 m line extending from the river edge towards the land (Figure 1e).

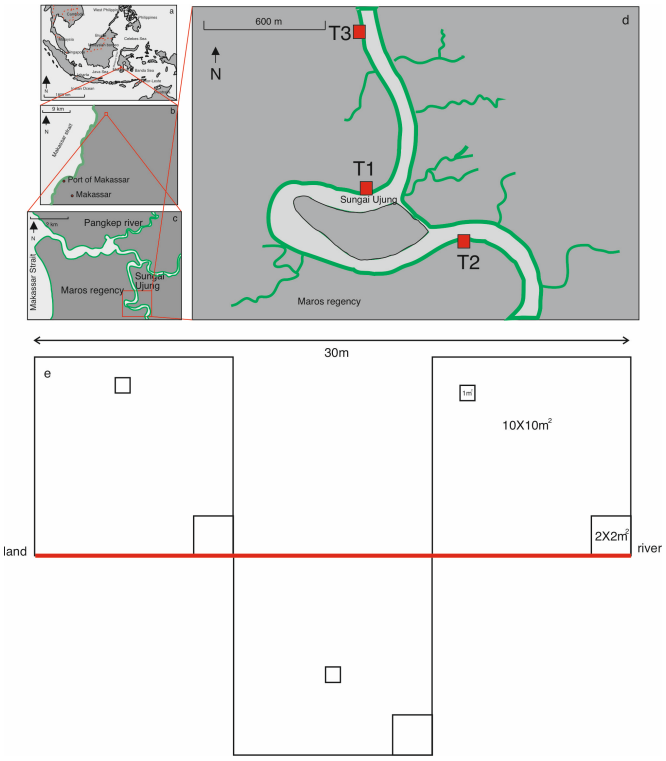


Figure 1. Study area and sampling design at Sungai Ujung River, Maros Regency, South Sulawesi, Indonesia. Panels (**a**–**d**) show the geographic location of the study area at different spatial scales: (**a**) the position of Sulawesi within the Indonesian archipelago; (**b**) the location of the study area relative to Makassar, the capital city of South Sulawesi Province; (**c**) the western part of Maros Regency; and (**d**) the sampling area at Sungai Ujung River. Red boxes indicate successive map enlargements, and the red squares mark the sampling locations T1–3: Transect 1–3. Green areas represent *Rhizophora mucronata*-dominated mangroves. Panel (**e**) illustrates the sampling design used for mangrove vegetation and intertidal crabs. Along each 30 m transect extending from the river edge toward the land, three 10 × 10 m plots were established for mangrove tree sampling (DBH > 10 cm). Within each main plot, one 2 × 2 m subplot was used for pole (DBH 2–10 cm) and seedling (DBH < 2 cm and height < 150 cm) sampling, and one 1 m^2 subplot was positioned randomly for surface-active crab sampling.

The initial field design consisted of three transects, with a target of three plots per transect, sampled during three spring-tide occasions and three neap-tide occasions. However, the mangrove belt was narrow in Transects 1 and 2, so only two plots could be established in each of these transects. Three plots were established only in Transect 3. In addition, one neap-tide sampling occasion could not be completed because of technical constraints. Therefore, the complete field dataset consisted of two plots in Transect 1, two plots in Transect 2, and three plots in Transect 3, sampled during three spring-tide occasions and two neap-tide occasions.

2.1. Surface-Active Crab Community

Surface-active crab sampling was restricted to epibenthic individuals visible on the sediment surface during low tide. Samples were collected from two 1 m^2 sub-plots within each transect (Figure 1e) following standard plot-based approaches for intertidal macrozoobenthos and brachyuran crabs [22–24]. Surface-active crab sampling used an adapted timed visual hand-collection approach informed by previous mangrove crab survey methods using timed visual or manual searches [25–27]. Each 1 m^2 subplot was surveyed for 45 min, during which all intact, visible, surface-active crabs encountered on the sediment surface and accessible root microhabitats were collected for identification. The 45 min duration was used as an extended observation period to improve detection of visible surface-active individuals and should not be interpreted as a standardized duration taken directly from a single reference. Because the method did not include burrow excavation, trapping, quadrat excavation, or intensive sediment searching, subterranean, cryptic, nocturnal, very small, damaged, or less active individuals were not systematically sampled. Sex was not determined because it was not relevant to the objectives of this study.

Captured individuals were temporarily maintained in aerated containers filled with ambient seawater to minimize handling stress during transport and identification [14]. Morphological identification was conducted using standard taxonomic references [28–34]. Following identification, all individuals were returned alive to their original collection sites within 48 h [14]. Selected individuals retained for molecular validation were not returned, but were preserved as voucher specimens and deposited in the Marine Biology Laboratory, Vrije Universiteit Brussel, Brussels, Belgium. In this study, "voucher specimen" refers to the retained physical specimen or preserved specimen material linked to the corresponding molecular sequence and specimen record.

To validate morphological identification, three individuals from each morphologically distinct group were selected for DNA barcoding. These individuals were distributed across transects, one individual per transect, to account for potential spatial variation in species identity and to ensure that morphological validation was not limited to a single sampling location. When a morphotype was absent from one or more transects, no specimen could be selected from the absent transect, and the available specimens were selected only from transects where that morphotype occurred. Voucher and specimen information, including morphotype code, specimen code, collection information, final taxonomic assignment, and GenBank accession number when available, is provided in Table A1.

Selected voucher specimens retained for molecular validation were rapidly immersed in ice-cold water to induce hypothermia and reduce activity, after which they were transferred to a freezer and stored at −20 °C until further measurement and analysis [35]. Subsequently, all samples were preserved in a refrigerator at −20 °C until further measurements and analyses. The pereiopod tips of each crab were extracted and then stored in a 1.5 mL microcentrifuge tube, then preserved directly in 96% ethanol. The samples were stored at −20 °C for further DNA barcoding analysis [36].

DNA extraction was conducted with approximately 3 mg of cheliped tissue following the Qiagen DNeasy Blood and Tissue Kit manufacturer's protocol. Extract quality was visually checked after gel electrophoresis under UV light. Successful DNA extractions were amplified using PCR targeting the mitochondrial cytochrome oxidase subunit I gene (COI) with the primers HCO 2198 and LCO 1490, targeting an approximately 710 base pairs (bp) COI fragment [37]. Final edited sequences retained after trimming were shorter. The PCR had a volume of 50 µL, composed of 25 µL of VWR Taq 2× Master Mix (VWR, Radnor, PA, USA), 1 µL of each forward and reverse primer (10 µM), 2 µL of 25 mM MgCl2, 20 µL of PCR-grade H_2O, and 1 µL of template DNA. The following protocol was used for amplification: initial denaturation at 95 °C for 3–5 min, followed by 35 cycles of (1) denaturation at 95 °C for 30 s, (2) annealing at 50 °C for 30 s, and (3) elongation at 72 °C for 1 min. Upon completion of these cycles, a final extension occurs at 72 °C for 10 min, followed by cooling down to 20 °C for 1 s. Electrophoresis using agarose gel was performed to assess the quality of the PCR product [36]. The PCR was conducted using the VWR peqSTAR 96× thermocycler (Avantor, Radnor, PA, USA). Amplicons were qualitatively and quantitatively checked using gel electrophoresis and a NanoDrop™ 2000/2000c Spectrophotometer (Thermo Fisher Scientific, Waltham, MA, USA) (acceptable A260/A280 ratio: 1.8–2.0; concentration $\geq$ 10 ng/µL). Qualified samples underwent sequencing with an ABI3730XL sequencer (Thermo Fisher Scientific, Waltham, MA, USA) at Macrogen (Amsterdam, The Netherlands). High-quality sequences generated in this study were deposited in the National Center for Biotechnology Information (NCBI) GenBank database.

2.2. Water Quality and Sediment Grain Size

Water salinity, pH, and total dissolved solids (TDS) were measured in situ from surface water at each plot using portable field instruments. Salinity was measured using a handheld salinorefractometer (Extech Instruments, Nashua, NH, USA) and reported using the salinity scale of the instrument. pH was measured using a portable pH meter (COM-600), and TDS was measured using a portable TDS meter. All instruments were calibrated or checked according to the manufacturers' instructions before field measurements. The salinorefractometer was checked with distilled water before use, while the pH and TDS meters were calibrated or checked using the corresponding standard solutions recommended for each instrument. TDS values were recorded from the meter display and multiplied by 10 because the instrument displayed values on a ×10 scale; final TDS values are therefore reported in ppm.

Surface sediment samples (100 g) were collected from each plot and analyzed for texture composition using the hydrometer method. The depth of sediment collection was 10 cm. The dispersion procedure followed the Rapid Method, where soil samples were dispersed using 3% sodium hexametaphosphate (HMP) and shaken for 2 h. Organic matter was not chemically removed. The Rapid Method uses a 0.053 mm mesh sieve to collect the sand fraction. Sand percentage is calculated from the oven-dry sand mass relative to original sample mass. The silt + clay suspension is stirred thoroughly, allowed to settle undisturbed at 18–24 °C for at least 90 min but less than 6 h, then suspended clay is decanted from settled silt. Sand and silt contents were calculated from oven-dry masses, while clay content was calculated by difference. Each transect-level composite sediment sample was analyzed once; therefore, laboratory replicate variability was not available [38]. Tidal periods were classified using lunar phase information and tide-prediction data from the Sistem Referensi Geospasial Indonesia/Badan Informasi Geospasial (SRGI/BIG) tide service. The nearest tide station used was Makassar (station code: UJPD), with water levels referenced to Mean Sea Level (MSL) and an indicated tidal range of approximately

1.2 m. Field timing was also cross-checked with local fishers to ensure safe and feasible sampling conditions.

2.3. Mangrove Stands Community

Mangrove trees, poles, and seedlings were counted along the same transects used for crab surveys, using 100 m^2 plots for trees and 4 m^2 plots for poles and seedlings (Figure 1e). They were identified to species level based on morphological characteristics using the global mangrove database [39]. Recorded variables included species, abundance, growth category (trees, poles, and seedlings), and diameter at breast height (DBH). DBH was measured 137 cm above the surface, and 30 cm above the highest visible root for *Rhizophora* spp. Seedlings were defined as living individuals with height < 150 cm and DBH < 2 cm. Poles were defined as individuals with DBH between 2 and 10 cm, and trees were defined as individuals with DBH >10 cm. Therefore, individuals with DBH between 2 and 10 cm were not omitted but were assigned to the pole category [12].

2.4. Molecular Sequence Processing and Data Analysis

Voucher specimens were deposited for each morphotype prior to molecular analysis. DNA sequencing was conducted using unidirectional sequencing of the COI amplicons. Raw chromatograms were inspected and edited using SnapGene v.3.8 (www.snapgene.com, (accessed on 17 July 2026). Low-quality terminal regions were trimmed manually based on chromatogram quality, and ambiguous base calls were checked against the original electropherogram peaks. When a base could not be confidently assigned because of overlapping or unclear peaks, the position was coded using the appropriate IUPAC ambiguity codes. The final edited single-read sequences were retained for downstream analysis only when the trimmed read showed sufficient chromatogram quality, no excessive ambiguous positions, and no ambiguous positions that affected taxonomic interpretation. The edited COI sequences were then translated into amino acids to verify the reading frame and screen for premature stop codons or obvious pseudogene-like sequences.

For each morphotype, the five to eleven highest-scoring reference sequences were retrieved from the corresponding database and used for subsequent phylogenetic validation (Table A2). When suitable reference sequences were unavailable in BOLD, additional reference sequences were retrieved from GenBank, recognizing that the two databases may contain overlapping sequence records. Sequences of *Scylla olivacea*, *S. tranquebarica*, *S. paramamosain* Estampador, 1950, and *S. serrata* (Forskål, 1775) were included as outgroups to root the phylogenetic tree (Table A3).

Reference, outgroup, and study sequences were compiled and aligned using MAFFT v7.526 through the command-line interface with the automatic alignment strategy [40]. The resulting alignment was trimmed to a common length prior to phylogenetic inference. Maximum-likelihood phylogenetic reconstruction was performed using IQ-TREE 3 v3.1.1 [41]. The best-fit nucleotide substitution model was selected using ModelFinder according to the Bayesian Information Criterion (BIC), which identified the transitional model with empirical base frequencies and a FreeRate model with two rate categories (TIM + F + R2) as the optimal model. Node support was assessed using 1000 bootstrap replicates. The resulting phylogeny was visualized and annotated using Interactive Tree Of Life (iTOL) v7.6 [42]. The final phylogenetic dataset included seven study sequences accepted after quality control and 29 reference or outgroup sequences, resulting in 36 sequences in total. After MAFFT alignment and trimming, the final alignment matrix contained 627 nucleotide columns and 404 distinct site patterns. This alignment length refers to the complete aligned matrix, not to the observed length of each study sequence. The accepted study sequences ranged from 560 to 597 bp; therefore, missing terminal positions in shorter sequences were

represented as terminal gaps and treated as missing data during maximum-likelihood phylogenetic reconstruction.

Final taxonomic assignments were determined by integrating morphological identification, sequence similarity searches against BOLD and GenBank databases, and phylogenetic clustering with reference sequences. Taxonomic units were assigned to genus or species level when supported by morphology, sequence similarity, and phylogenetic placement. Assignments with insufficient molecular resolution or unsuitable sequence quality were retained at the lowest reliable morphological level, including family level where appropriate.

Community diversity for surface-active crabs was calculated using Formula 1 [43], where pi represents the proportional abundance of each taxonomic unit. DBH of mangrove trees was calculated from stem circumference (Formula 2), and Basal Area (BA) was subsequently derived from DBH values (Formula 3) [44].

$$H = -\Sigma[pi * \ln(pi)] \quad (1)$$

$$DBH = \frac{\text{stem circumference}}{\pi} \quad (2)$$

$$BA = \pi \times \left(\frac{DBH}{2}\right)^2 \quad (3)$$

For surface-active brachyuran crabs, all valid plot-level observations were retained, including Transect 3 Plot 3 and the third spring-tide sampling occasion. The final crab dataset was structured as plot × sampling occasion observations, with seven plots sampled across five valid sampling occasions: three spring-tide occasions and two neap-tide occasions. Because tidal period was a sampling-occasion-level condition, plots sampled on the same date were treated as spatial subsamples within each sampling occasion rather than as independent temporal replicates. Therefore, no inferential spring–neap comparison was performed.

Surface-active brachyuran assemblages were summarized descriptively. Full-survey abundance was calculated by pooling all valid observations across plots and sampling occasions for each taxonomic unit. Sampling-occasion-level summaries were then calculated to describe total abundance and relative abundance of each taxonomic unit across the five valid sampling occasions. Plot-level assemblage metrics were calculated for each plot × sampling occasion observation, including total abundance, taxonomic-unit richness, Shannon diversity index, dominant taxon, and dominant taxon abundance. These metrics were used to describe within-occasion spatial variation and occasion-specific assemblage patterns. Spring and neap labels were retained only to describe the observed dry-season sampling occasions, not to infer general tidal-period effects.

The same sampling-occasion framework was applied to the water-quality variables. Salinity, pH, and total dissolved solids were retained as plot-level observations within each sampling occasion and summarized descriptively using mean, median, minimum, maximum, and standard deviation values. Because only three spring-tide occasions and two neap-tide occasions were available, temporal replication was insufficient for robust inferential testing of general spring–neap tidal effects. Therefore, water-quality patterns were interpreted descriptively at the sampling-occasion level. A principal component analysis (PCA) was conducted on standardized salinity, pH, and TDS values to visualize multivariate variation in plot-level water-quality profiles. The PCA was used as an exploratory descriptive ordination rather than as an inferential test of tidal-period differences.

Vegetation variables were analyzed descriptively because vegetation was surveyed once and had no temporal replication. Living stand density was calculated separately for each growth category using the corresponding sampled area: 100 m^2 for trees and 4 m^2

for poles and seedlings. Density was expressed as individuals m^{-2} and individuals ha^{-1}. Stand basal area was calculated at plot level for trees and poles using the sampled area corresponding to each growth category. Individual basal area was calculated from DBH, and plot-level stand basal area was expressed as m^2 ha^{-1}. Vegetation density and stand basal area were summarized across the seven surveyed plots and interpreted descriptively.

Sediment texture was also analyzed descriptively. Because sediment samples were composited by transect before laboratory analysis, sediment texture was summarized at the transect level as the percentage composition of sand, silt, and clay. No inferential comparison among transects was performed. All analyses were conducted using R version 4.2.3 [45]. The following package versions were used: readxl 1.5.0, tidyverse 2.0.0, ggplot2 3.5.1, dplyr 1.2.1, tidyr 1.3.2, readr 2.1.5, purrr 1.2.2, tibble 3.3.1, stringr 1.6.0, and forcats 1.0.1 [46–54].

3. Results

3.1. Sampling Hierarchy

The final descriptive dataset reflected the actual field sampling structure rather than a balanced complete-case subset. The original field design aimed to sample three transects, with three plots per transect, across three spring-tide and three neap-tide occasions. However, because the mangrove belt was narrow in Transects 1 and 2, only two plots could be established in each of these transects. Three plots were established in Transect 3. Therefore, seven vegetation and crab-sampling plots were included in the final descriptive dataset: two plots in Transect 1, two plots in Transect 2, and three plots in Transect 3.

For surface-active brachyuran crabs and water-quality variables, five valid sampling occasions were available: three spring-tide occasions and two neap-tide occasions. One planned neap-tide sampling occasion could not be completed because of technical constraints and was therefore not included in the analysis. The final crab and water-quality datasets were therefore structured as plot × sampling occasion observations, with plots treated as spatial subsamples within each sampling occasion. Because tidal period was a sampling-occasion-level condition, plots sampled on the same date were not treated as independent temporal replicates of spring or neap conditions.

Accordingly, no inferential spring–neap comparisons were performed. Instead, surface-active brachyuran assemblage patterns and water-quality variables were summarized descriptively across the five valid sampling occasions. Vegetation variables were measured once and interpreted as plot-level descriptive variables across the seven surveyed plots. Sediment texture was interpreted at the transect level because sediment samples were composited by transect before laboratory analysis (Table 1).

Table 1. Sampling hierarchy of the final descriptive dataset used in this study, showing the actual number of transects, plots, valid sampling occasions, and analytical interpretation for each dataset component.

Dataset Component	Spatial Level	Temporal Level	Final Observations Used	Analytical Interpretation
Surface-active brachyuran crabs	7 plots across 3 transects	5 valid sampling occasions: 3 spring, 2 neap	Plot × sampling occasion observations	Descriptive summary of abundance, taxonomic composition, Shannon diversity, and richness across sampling occasions
Water quality variables	7 plots across 3 transects	5 valid sampling occasions: 3 spring, 2 neap	Plot × sampling occasion observations	Descriptive summary and PCA of plot-level water-quality profiles

Table 1. *Cont.*

Dataset Component	Spatial Level	Temporal Level	Final Observations Used	Analytical Interpretation
Vegetation structure	7 plots across 3 transects	Single vegetation survey	Plot-level observations	Descriptive summary of area-standardized density and stand basal area
Sediment texture	3 transect-level composite samples	Single sediment survey	Transect-level composite observations	Descriptive summary of sediment texture composition among transects

Thus, the independent temporal level for crab and water-quality data was the sampling occasion/date, not the plot. Plot-level observations were used to describe within-occasion spatial heterogeneity, but were not used as independent replicates for testing general spring–neap tidal effects.

3.2. Surface-Active Brachyuran Taxonomic Unit Assemblages

Taxonomic identification of surface-active brachyuran crabs was based on two levels of evidence: morphological identification and, where successful, morphological identification supported by COI DNA barcoding. Because DNA barcoding success varied among morphologically defined groups, not all taxonomic units could be resolved to the same taxonomic level. Some units were identified only to family level based on morphology, whereas others were validated to genus or species level using DNA barcoding (Figure A1). Therefore, the recorded groups are referred to as taxonomic units rather than species-level taxa throughout this study.

Two morphologically distinct units, coded B and F, were assigned to the family Sesarmidae Dana, 1851 and Gecarcinidae MacLeay, 1838, respectively, based on morphological characteristics. The resulting sequences showed low similarity to available database records, inconsistent taxonomic matches, and unstable phylogenetic placement. These sequences were therefore excluded from molecular taxonomic validation.

In contrast, morphotype H was successfully resolved to species level and assigned to *Metopograpsus latifrons* (White, 1847). Although the BOLD search supported *M. latifrons* while the highest GenBank matches indicated *M. oceanicus*, the final assignment was based on the combined evidence from BOLD, phylogenetic placement, and comparison of diagnostic morphological characters with published descriptions of *M. latifrons* and *M. oceanicus* [55,56]. The study sequence grouped with *M. latifrons* reference sequence in the phylogenetic tree (Figure A1), and the specimen morphology showed closer agreement with published descriptions of *M. latifrons*, particularly in the coloration and structure of the walking legs and chelae. On this basis, we retained the assignment as *M. latifrons* rather than treating it as an unequivocally validated species-level record.

Based on this integrative identification approach, the surface-active brachyuran dataset comprised eight taxonomic units and 676 individuals (Tables 2, A1 and A4). Abundance was unevenly distributed among taxonomic units. *M. latifrons* was the most consistently recorded and abundant taxonomic unit across tidal periods, whereas the remaining taxonomic units occurred at lower abundance and were more restricted to particular plots or tidal periods. Because the dataset included family-, genus-, and species-level assignments, assemblage composition and diversity were interpreted at the taxonomic-unit level rather than as species-level crab diversity.

Table 2. List of surface-active taxonomic units recorded in this study. *: identification based on morphological characteristics and DNA barcoding; ** identified based on morphology only due to unsuccessful DNA extraction or poor DNA sequence quality.

Morphotype Code	Total Individuals	Taxonomic Unit Identity	Family
A	23	Sesarmidae Dana, 1851 morphotype 1 **	Sesarmidae
B	10	Sesarmidae Dana, 1851 morphotype 2 **	Sesarmidae
C	47	Parasesarma De Man, 1895 *	Sesarmidae
D	8	Ocypodidae Rafinesque, 1815 morphotype 1 **	Ocypodidae
E	36	Ocypodidae Rafinesque, 1815 morphotype 2 **	Ocypodidae
F	82	Gecarcinidae MacLeay, 1838 **	Gecarcinidae
G	56	*Metaplax elegans* De Man, 1888 *	Varunidae
H	414	*Metopograpsus latifrons* (White, 1847) *	Grapsidae

Across the full survey, surface-active brachyuran abundance was unevenly distributed among taxonomic units. *Metopograpsus latifrons* was the dominant taxonomic unit, contributing the largest proportion of recorded individuals across the study period. Other taxonomic units occurred at substantially lower abundance, including Gecarcinidae (Figure 2), *Metaplax elegans* De Man, 1888, Parasesarma De Man, 1895, Ocypodidae Rafinesque, 1815, and Sesarmidae taxonomic units. This pattern indicates that the visible low-tide brachyuran assemblage was strongly dominated by one surface-active grapsid crab, while the remaining taxonomic units formed a smaller and more variable component of the assemblage.

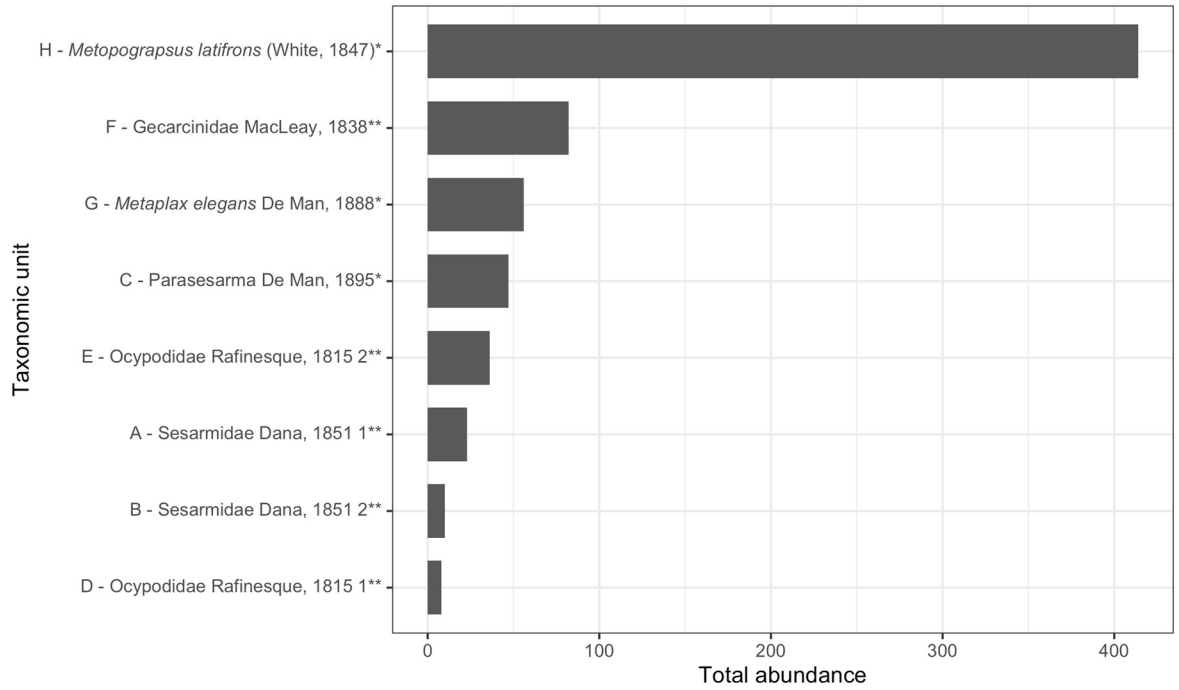


Figure 2. Full-survey abundance of surface-active brachyuran taxonomic units recorded in the replanted *Rhizophora mucronata* stand. Abundance was pooled across all sampled plots and five valid sampling occasions, comprising 676 individuals from eight taxonomic units. *: identification based on morphological characteristics and DNA barcoding; ** identified based on morphology only due to unsuccessful DNA extraction or poor DNA sequence quality.

When abundance was summarized by sampling occasion, total abundance varied among dates rather than showing a simple or consistent spring–neap pattern (Figure 3). *Metopograpsus latifrons* dominated the first two sampling occasions, particularly Spring 1 and Neap 1, where most recorded individuals belonged to this taxonomic unit. In later sampling occasions, the assemblage became more compositionally mixed, with greater contributions from Gecarcinidae, *M. elegans*, Parasesarma, Ocypodidae, and Sesarmidae taxonomic units. This shift was also visible in the relative-abundance plot, where early occasions were almost entirely dominated by *M. latifrons*, whereas later occasions showed a more even distribution among several taxonomic units.

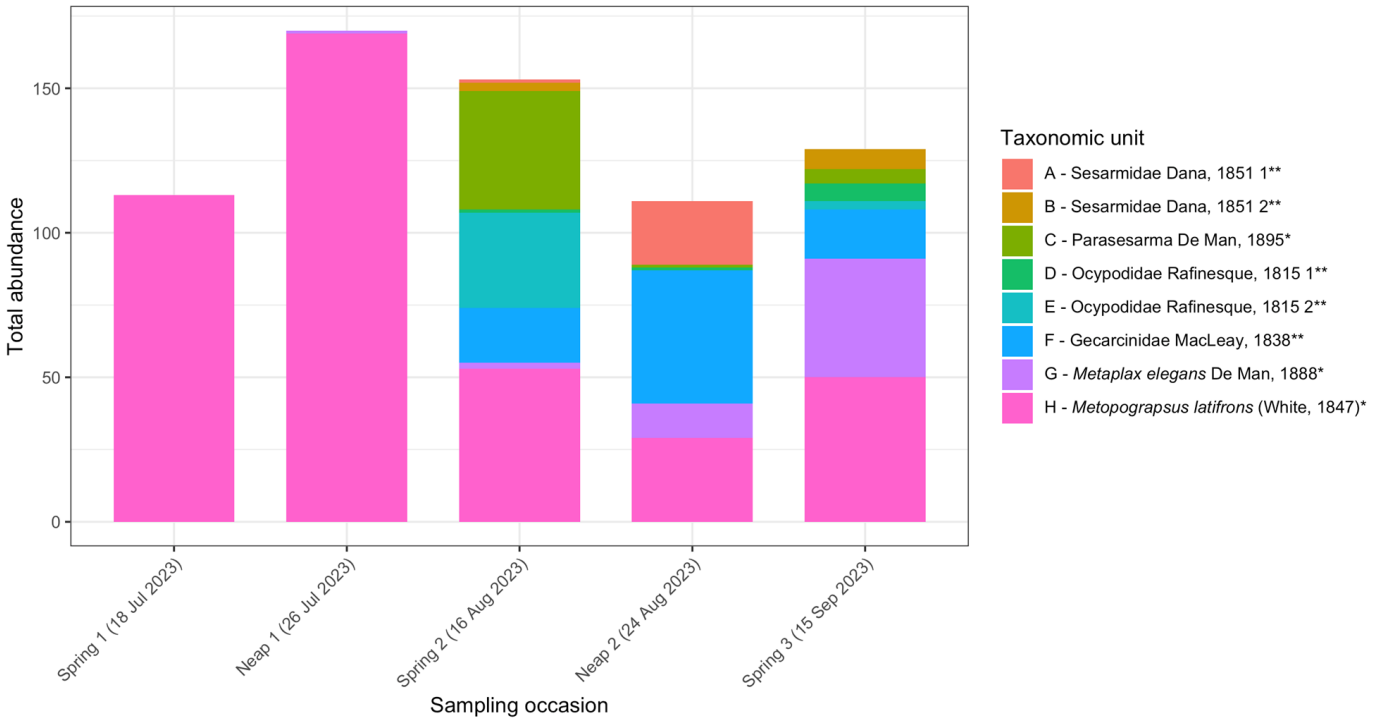


Figure 3. Surface-active brachyuran taxonomic-unit abundance by sampling occasion. Bars show total abundance pooled across sampled plots within each of the five valid sampling occasions, based on the full descriptive crab dataset of 676 individuals and eight taxonomic units. *: identification based on morphological characteristics and DNA barcoding; ** identified based on morphology only due to unsuccessful DNA extraction or poor DNA sequence quality.

Plot-level total abundance also varied within and among sampling occasions (Figure 4). Median plot-level abundance was broadly comparable across the five occasions, but individual plots showed substantial variation, including one high-abundance plot during Neap 1. This indicates that spatial variation among plots within the same sampling occasion was considerable. Therefore, plot-level variation should be interpreted as within-occasion spatial heterogeneity rather than as independent temporal replication of tidal period.

Plot-level Shannon diversity and taxonomic-unit richness showed similar descriptive patterns (Figure 5). The first two sampling occasions had low richness and low Shannon diversity in most plots, reflecting the strong dominance of *M. latifrons*. In contrast, later occasions, especially Spring 2, Neap 2, and Spring 3, showed higher richness and Shannon diversity in several plots, indicating greater representation of multiple taxonomic units. However, values still varied substantially among plots within the same occasion. Overall, these results suggest occasion-specific and plot-level variability in the surface-active brachyuran assemblage, rather than a clear general spring–neap separation.

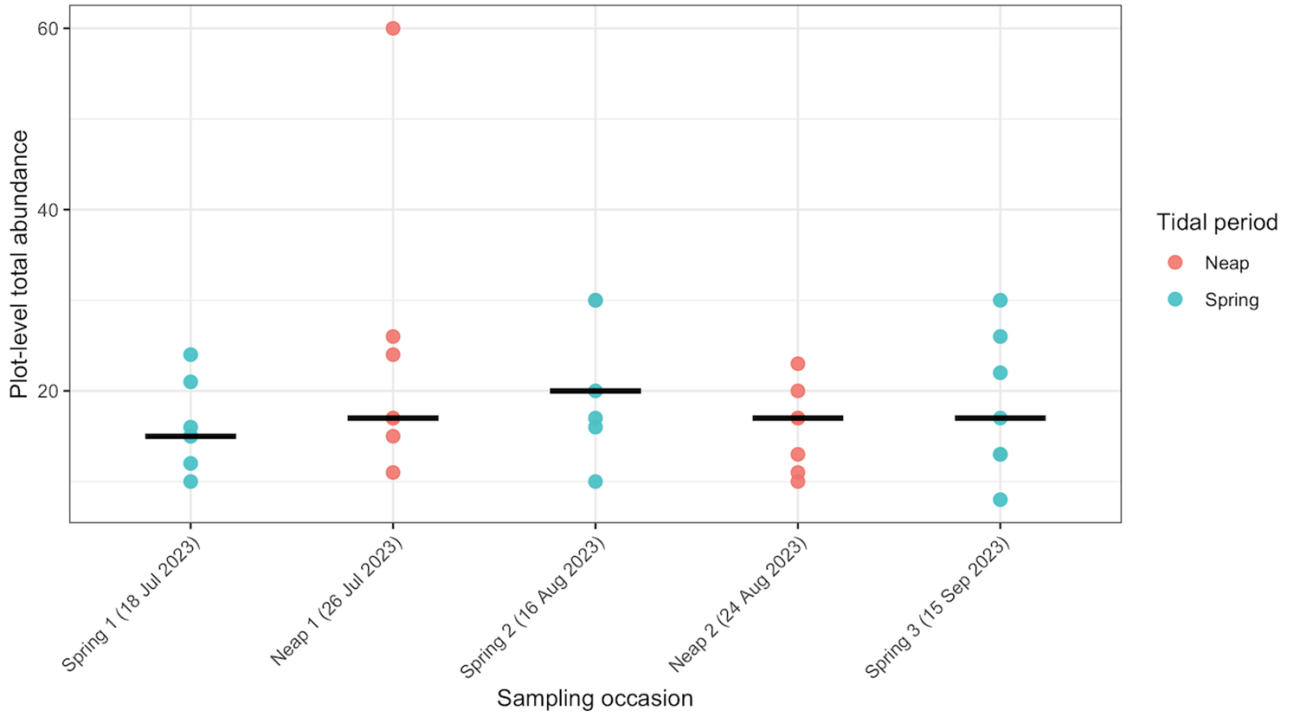


Figure 4. Plot-level total abundance of surface-active brachyuran crabs by sampling occasion. Points represent plot × sampling occasion observations from the descriptive crab subset, and black crossbars indicate median plot-level abundance for each occasion. Colors indicate tidal period.

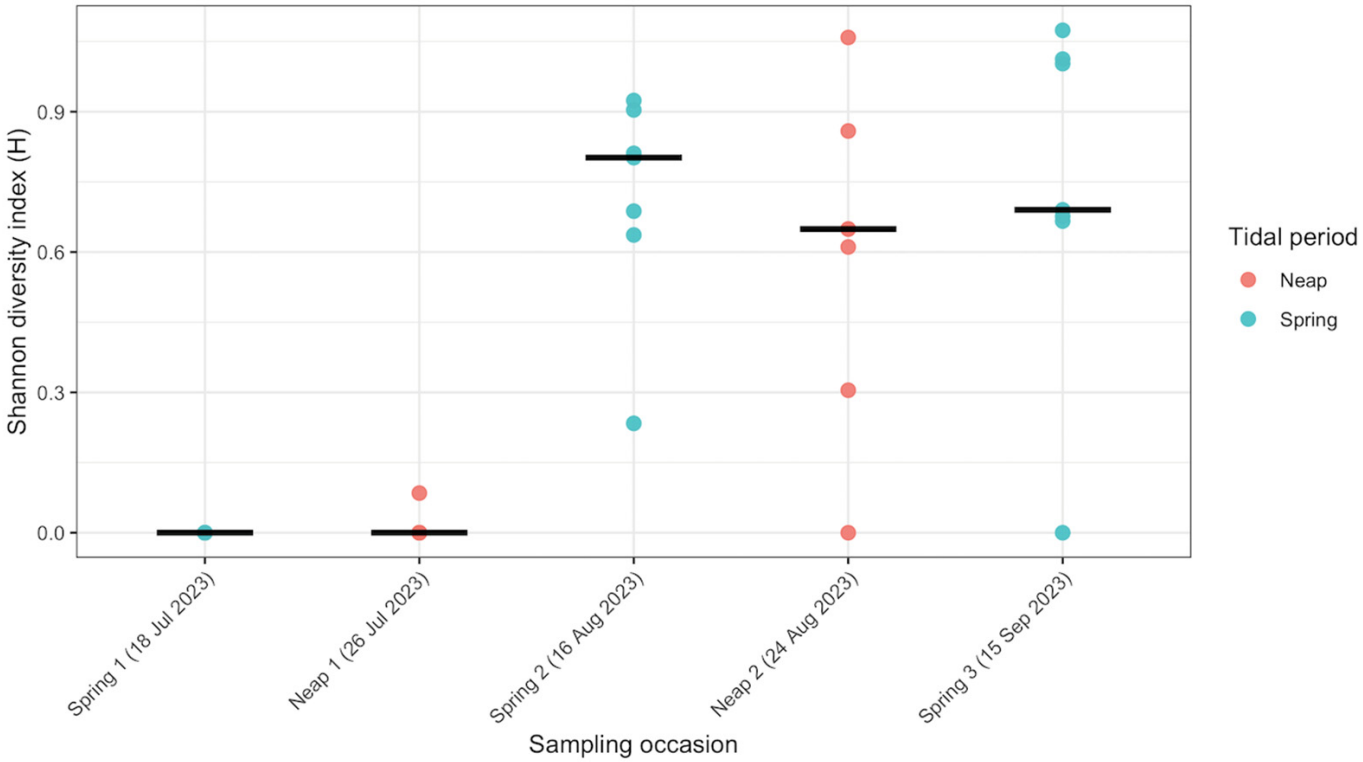


Figure 5. Plot-level Shannon diversity of surface-active brachyuran crabs by sampling occasion. Points represent plot × sampling occasion observations from the descriptive crab subset, and black crossbars indicate median plot-level Shannon diversity for each occasion. Colors indicate tidal period.

3.3. Selected Water-Quality Variables

Plot-level water-quality variables varied across the five valid sampling occasions (Figure 6; Table A5). Salinity and TDS showed broadly similar patterns, with lower values during the first neap occasion and higher values during later spring occasions, particularly Spring 2 and Spring 3. In contrast, pH varied within a narrower range and tended to be lower during Spring 2 and Spring 3 than during the earlier occasions. However, plot-level values also varied within the same sampling occasion, indicating spatial heterogeneity among plots sampled under the same tidal event.

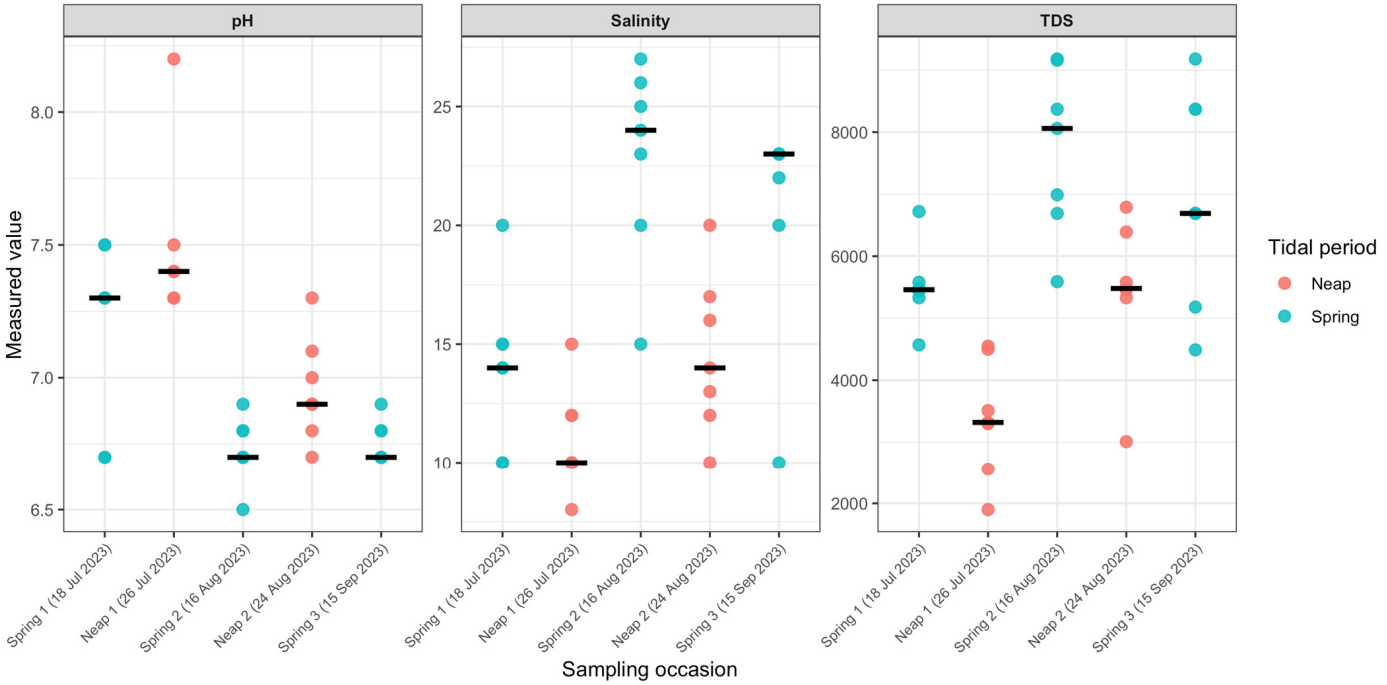


Figure 6. Plot-level water-quality variables across five valid sampling occasions in the replanted *Rhizophora mucronata* stand. Points represent plot × sampling occasion observations for surface-water pH, salinity, and TDS (n = 35 per variable; seven plots across five occasions), and black crossbars indicate median plot-level values for each occasion. Colors indicate tidal period.

The descriptive PCA supported these patterns (Figure 7). The first two principal components explained 93.03% of the variation in standardized water-quality profiles, with PC1 explaining 76.16% and PC2 explaining 16.87%. PC1 was positively associated with salinity and TDS and negatively associated with pH, indicating a gradient from lower salinity/TDS and higher pH toward higher salinity/TDS and lower pH. Spring samples, especially from later sampling occasions, tended to occur toward higher PC1 scores, while several neap samples occurred toward lower PC1 scores. Nevertheless, because sampling occasions were limited and plots were spatial subsamples within occasions, the PCA was interpreted descriptively rather than as evidence of a general inferential spring–neap tidal effect.

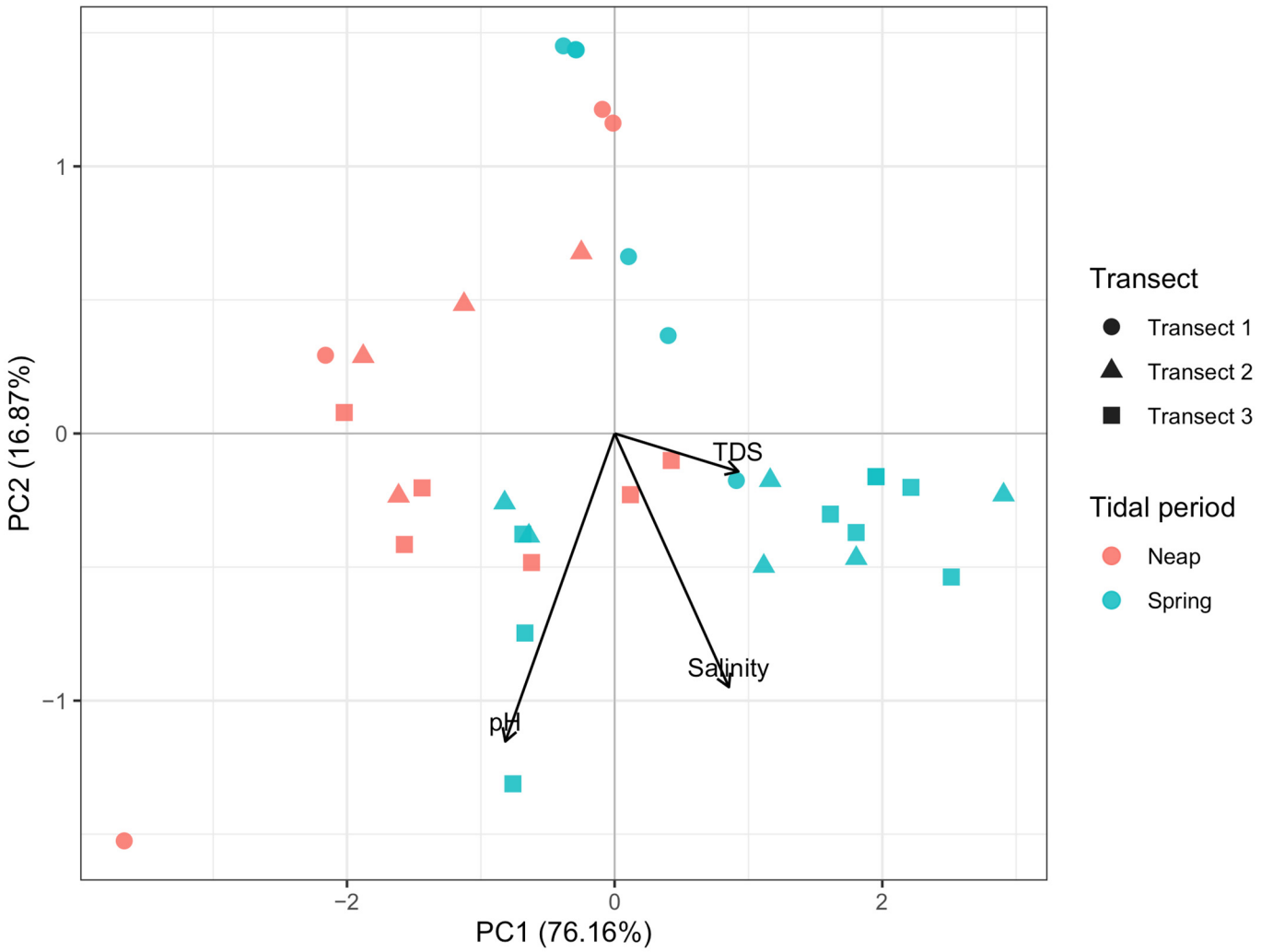


Figure 7. PCA biplot of standardized plot-level water-quality profiles across five valid sampling occasions. Points represent plot × sampling occasion observations with complete pH, salinity, and TDS measurements (n = 35), colors indicate tidal period, and shapes indicate transects. Arrows show variable loadings. PC1 explained 76.16% of the variation and was positively associated with salinity and TDS and negatively associated with pH, while PC2 explained 16.87%.

3.4. Mangrove Vegetation Structure Among Transects

Area-standardized density varied among growth categories and transects (Figure 8). Seedlings showed the highest density across all transects, followed by trees, while pole-stage individuals were sparse. At the transect level, seedling density was highest in Transect 2, followed by Transect 1 and Transect 3. Tree density was also highest in Transect 2, while Transects 1 and 3 showed slightly lower values. In contrast, pole density was low overall and was recorded only in Transects 1 and 3, with no pole-stage individuals recorded in Transect 2.

Plot-level stand basal area varied among plots and growth categories (Figure 9). Tree basal area was recorded across all seven surveyed plots, indicating the presence of an established living *R. mucronata* tree layer within the replanted stand. However, tree basal area was not uniform across the site, with some plots showing substantially higher values than others, reflecting plot-level variation in stand structure. Pole basal area was much more limited. Measurable pole basal area occurred only in a small number of plots, while most plots had no recorded pole-stage basal area.

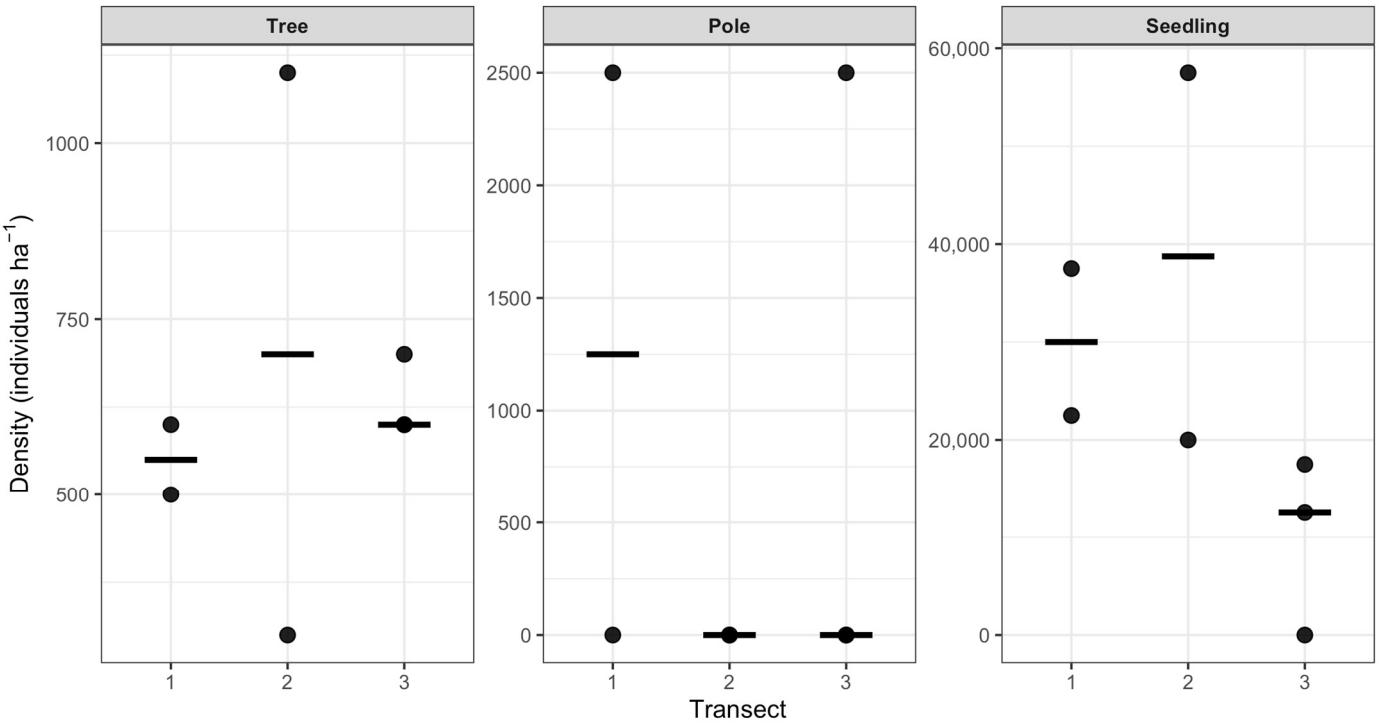


Figure 8. Plot-level area-standardized density of living *Rhizophora mucronata* individuals by growth category and transect. Points represent plot-level densities for each growth category (n = 7 plots per category: two plots in Transects 1 and 2, and three plots in Transect 3), and black crossbars indicate median plot-level density within each transect. Density was calculated using the sampled area for each growth category: 100 m^2 for trees and 4 m^2 for poles and seedlings, then expressed as individuals ha^{-1}.

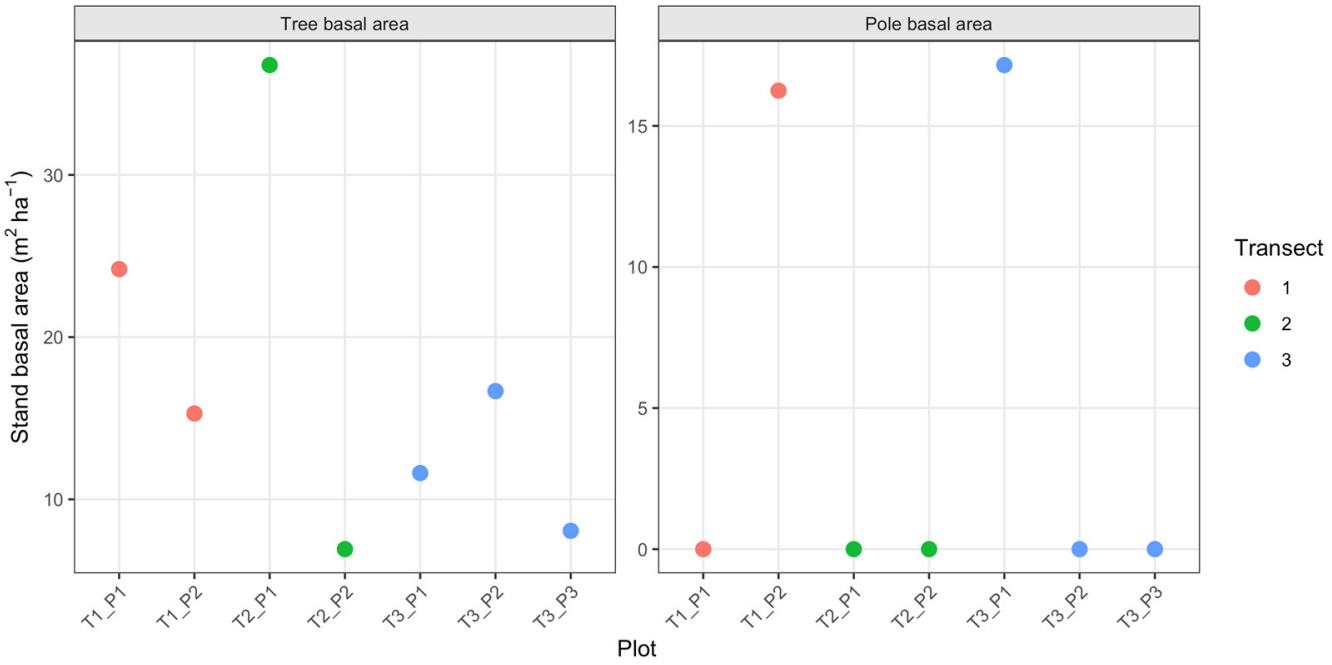


Figure 9. Plot-level stand basal area of living *Rhizophora mucronata* by growth category and transect. Points represent individual plot-level observations from seven surveyed vegetation plots: two plots in Transect 1, two plots in Transect 2, and three plots in Transect 3. Black crossbars indicate median plot-level stand basal area within each transect. Tree basal area was calculated from 100 m^2 plots, whereas pole basal area was calculated from 4 m^2 subplots; values are expressed as m^2 ha^{-1}.

3.5. Sediment Texture Among Transects

Sediment texture differed descriptively among transects (Figure 10). Transect 1 was dominated by sand, which accounted for 60% of the sediment composition, followed by clay (25%) and silt (15%). In contrast, Transects 2 and 3 were dominated by finer sediment fractions, particularly clay, which accounted for 54% and 59% of the sediment composition, respectively. Sand content decreased from 60% in Transect 1 to 23% in Transect 2 and 19% in Transect 3, while clay content increased across the same transect sequence. Because sediment samples were composited by transect before laboratory analysis, these values were interpreted descriptively, and no inferential comparison among transects was performed.

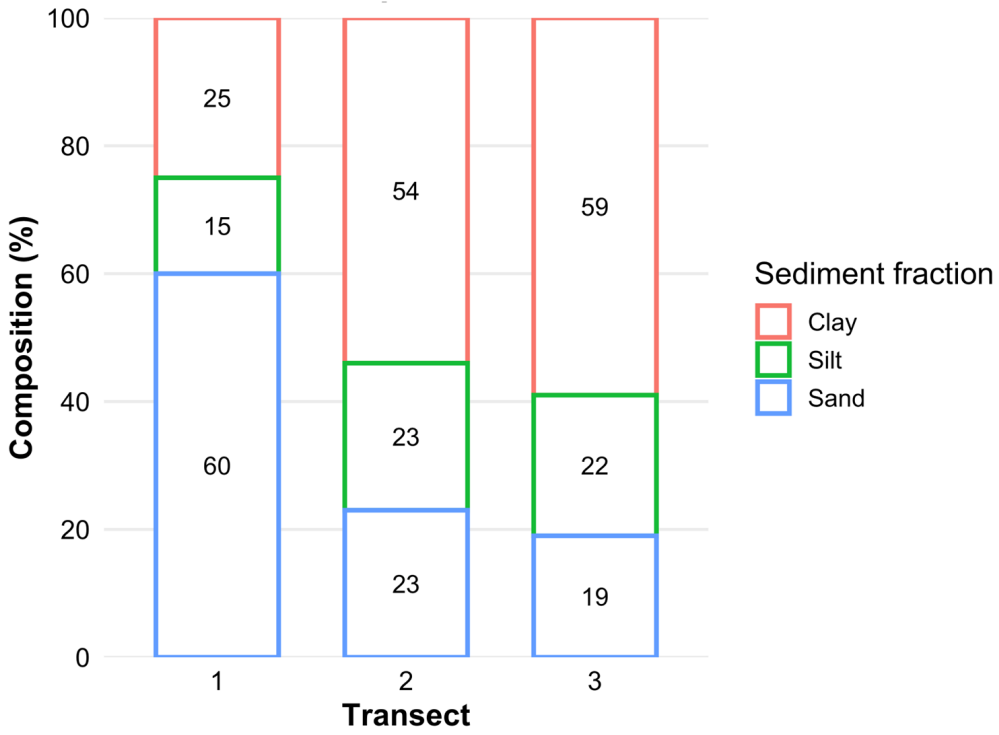


Figure 10. Sediment texture composition across transects in the replanted mangrove stand at Sungai Ujung River, South Sulawesi, Indonesia. Bars show the proportional contribution (%) of sand, silt, and clay in each transect-level sediment sample.

4. Discussion

This study provides a dry-season, post-plantation habitat characterization of an eight-year-old replanted *R. mucronata* stand at Sungai Ujung River, rather than an evaluation of replantation success, recovery assessment, or rehabilitation trajectory. The absence of a pre-plantation baseline, early post-plantation observations, long-term monitoring data, and comparable natural or unrestored reference sites prevents estimation of the direction, rate, and completeness of ecological change, as well as attribution of the present conditions specifically to the planting intervention. A global meta-analysis showed that restored mangroves generally supported greater ecosystem functioning than unvegetated tidal flats but lower functioning than natural mangrove forests, with substantial variation among functions and restoration contexts [57]. Moreover, inconsistent reporting of pre-restoration site conditions has been identified as a major limitation to comparisons among mangrove restoration projects [58]. In Sulawesi, Indonesia, even 14–16-year-old monoculture plantations continued to reflect their original planting configuration and remained structurally and compositionally distinct from reference forests [9]. Stand age alone should therefore

not be treated as evidence of ecological recovery. Accordingly, the present dataset is most appropriately interpreted as a site-specific snapshot of the vegetation, visible brachyuran fauna, and selected environmental conditions prevailing during the surveyed dry season.

4.1. Surface-Active Brachyuran Assemblages

Metopograpsus latifrons was the dominant taxonomic unit and contributed the largest proportion of recorded individuals, whereas Gecarcinidae, *Metaplax elegans*, *Parasesarma*, Ocypodidae, and Sesarmidae occurred at substantially lower abundances. This pattern indicates that the visible low-tide assemblage within the replanted stand was numerically dominated by one surface-active grapsid crab, with the other recorded taxonomic units forming smaller and more variable components. Nevertheless, the observations should not be interpreted as representing the entire resident brachyuran community. Surface-observation methods preferentially detect individuals that emerge and remain visible during the sampling window, while cryptic, nocturnal, arboreal, root-dwelling, or burrow-retreating taxa may be underestimated. Photographic surveys of tropical intertidal crabs similarly provided high spatial replication but did not represent the complete crab community when compared with complementary hand collections [59]. In addition, because the present dataset contains taxonomic units identified at different ranks (species, genus, and family), the calculated richness and diversity represent taxonomic-unit diversity rather than strictly species-level diversity. Turnover among species within the family-level categories would consequently remain unresolved. The dominance of *M. latifrons* is ecologically plausible within a structurally developed Rhizophora stand. Across low-intertidal habitats in tropical Australia, *M. latifrons* was associated with areas in which at least 22% of the substratum contained structural elements, indicating a strong relationship between this species and habitat complexity [5]. Although that quantitative threshold cannot be transferred directly to Sungai Ujung River, the finding supports the hypothesis that the prop–root matrix, woody material, and other structural features of the replanted stand may provide refuges, climbing surfaces, feeding areas, or protection from predators and tidal disturbance.

More broadly, mangrove-associated crabs, particularly grapsoid, sesarmid, and ocypodid taxa, can contribute to litter fragmentation and retention, trophic transfer, propagule consumption, sediment excavation, burrow formation, sediment aeration, and the redistribution of organic matter and nutrients [6]. However, these functions depend on species identity, body size, feeding behavior, burrow architecture, population biomass, and activity rate; they cannot be inferred reliably from numerical abundance alone. The present study did not quantify litter consumption, feeding rates, burrow density or geometry, sediment turnover, organic-matter burial, or nutrient fluxes. Consequently, the high abundance of *M. latifrons* demonstrates numerical dominance within the observed surface-active assemblage but does not establish functional dominance, enhanced ecosystem functioning, or habitat recovery.

When abundance was summarized by sampling occasion, total abundance and taxonomic composition varied among dates rather than following a simple and consistent spring–neap pattern. *M. latifrons* dominated the first two occasions, whereas later occasions contained a more compositionally mixed assemblage with greater representation of several lower-abundance taxonomic units. These results indicate that the assemblage visible at the sediment surface was not temporally uniform during the dry-season survey. Importantly, counts of surface-active crabs represent a combination of local abundance, availability for observation, and detection probability. Experimental observations of another semi-terrestrial mangrove crab, *Ucides cordatus* (Linnaeus, 1763), demonstrated that surface activity can vary with tidal inundation, daylight, lunar phase, season, litter availability, and

the presence of conspecifics [60]. Although responses observed for *U. cordatus* should not be assumed to apply directly to *M. latifrons* or the other taxa recorded here, they illustrate how behavioral variation can generate substantial differences in surface counts without equivalent changes in population size. Surface emergence and burrow dynamics can also respond to sediment temperature, rainfall, salinity, vegetation cover, and sediment physical properties [61]. Thus, the occasion-specific variation observed at Sungai Ujung River may reflect changes in activity, detectability, sediment moisture, microhabitat use, or other unmeasured conditions rather than short-term changes in the resident population.

Shannon diversity values were low during the first two occasions, largely because of the strong numerical dominance of *M. latifrons*, but became higher and more variable among plots during later occasions. Because the Shannon index is influenced by both richness and evenness, these increases do not necessarily indicate the establishment of additional resident taxa; they may partly reflect a more even distribution of the taxonomic units detected during those sampling windows. The high-abundance plot should similarly be interpreted as localized aggregation or elevated surface activity unless its recurrence can be demonstrated through repeated sampling.

Fine-scale variation in brachyuran distribution is expected in mangroves because adjacent patches can differ in root density, structural complexity, sediment grain size and compaction, organic-matter content, moisture retention, canopy cover, microtopography, inundation duration, and distance from tidal channels. Habitat modeling has demonstrated species-specific associations between intertidal crabs and substrate structure [62], while analyses of developing mangrove stands have identified sediment properties as important determinants of initial brachyuran establishment and have associated Rhizophora prop-root habitats with greater crab richness [63]. Crab burrow density and renewal can also vary spatially with sediment bulk density, particle size, salinity, sediment temperature, vegetation cover, and position relative to the river [61]. These findings provide plausible mechanisms for the plot-to-plot variability observed at Sungai Ujung River. Nevertheless, because crab abundance and composition were not statistically modeled against plot-level vegetation and environmental variables, none of these mechanisms can presently be identified as the cause of the observed spatial patterns.

Long-term comparative studies further demonstrate why the current assemblage should not be used independently as evidence of rehabilitation status. Comparisons among plantations of different ages and mature reference forests in Malaysia and Thailand found that crab community composition varied with management history and stand age, with ocypodids more prominent in young plantations and sesarmids more characteristic of mature forests [64]. More recent monitoring in Ranong, incorporating repeated surveys in 1999, 2008, and 2019 and comparison with a mixed-species conservation forest, likewise showed persistent differences among sites and proposed particular crab groups as context-dependent indicators of habitat development [25]. Those conclusions were possible because the studies included temporal replication, contrasting rehabilitation histories, and reference forests. The present study lacks these comparative dimensions, and its assemblage does not necessarily conform to a universal sequence of faunal succession. The occurrence or dominance of any individual taxon should therefore not be assigned an indicator meaning without local validation.

4.2. Vegetation Structure

All 113 living mangrove individuals recorded in the surveyed plots were identified as *R. mucronata*, indicating taxonomic uniformity within the sampled stand and a composition that continues to reflect the species used in the original planting intervention. The observed monospecific composition is consistent with the plantation context but should not, in the

absence of an appropriate natural reference, be interpreted as either a positive or negative indicator of ecological condition. Rather, it provides a descriptive characterization of the vegetation composition at the time of sampling. Planted mangrove forests can retain the floristic signature of their original planting design for extended periods. In the Philippines, monospecific plantations remained structurally less complex than adjacent natural stands, and one approximately 60-year-old plantation still showed limited understory recruitment and colonization by non-planted species [65]. Similarly, monoculture reforestation stands in Sulawesi remained strongly influenced by their planted foundation species and differed from reference forests in diversity and structure 14–16 years after intervention [66] Djamaluddin et al., 2019. Taxonomic uniformity at Sungai Ujung should therefore be interpreted as evidence of persistent planted composition, not as evidence of either degradation or recovery.

The density and growth-category composition indicated that seedlings were conspicuous components of the stand, particularly in Transects 1 and 2, where they constituted the largest proportion of recorded individuals. However, seedling abundance represents only the presence of an early demographic stage and does not demonstrate successful regeneration. A one-year study of more than 2,800 mangrove seedlings in Southeast Asia found that environmental controls on survival following establishment differed from those influencing initial propagule establishment, with light exerting a particularly strong effect on established seedlings [67]. Consequently, a high seedling density at one sampling time cannot be assumed to translate into an equivalent contribution to the future tree layer.

Pole-stage individuals were scarce and occurred only in Transects 1 and 3, while none were recorded in Transect 2 despite its relatively high seedling and tree densities. This produced an uneven size-class distribution consisting of an established tree layer, abundant seedlings in some plots, and weak representation of the intermediate growth category. Growth categories defined by size are demographic states rather than known age cohorts; the seedlings, poles, and trees observed during the survey cannot be assumed to represent a single cohort progressing sequentially through time. Thus, the scarcity of poles identifies a discontinuity in the current size-class structure but does not by itself demonstrate a recruitment bottleneck.

The basal-area results complement the density data by describing the cumulative cross-sectional area of the pole and tree components. Tree basal area was recorded in every surveyed plot, supporting the conclusion that an established living tree layer was present throughout the sampled stand. Nevertheless, tree basal area varied substantially among plots. The highest and lowest values occurred in different plots within Transect 2, demonstrating that structural development was heterogeneous even at the within-transect scale. Because basal area is determined jointly by stem abundance and diameter, a relatively high value can result from many moderately sized stems, a small number of large stems, or a combination of both. Pole basal area was recorded in only a limited number of plots, consistent with the low pole density.

Taken together, the vegetation data describe a monospecific replanted *R. mucronata* stand with an established but spatially heterogeneous tree layer, visible seedling establishment, and limited pole-stage representation. The data, however, cannot establish whether stand structure is moving toward, remaining different from, or diverging from a desired reference condition. Restoration literature increasingly emphasizes that survival and planted area alone are insufficient indicators. Vegetation structure, compositional diversity, environmental conditions, intervention history, and comparison with an explicitly defined reference system are necessary for evaluating progress and durability [2,9].

4.3. Water Quality Variables and Sediment Texture

Plot-level surface-water variables varied across the five valid sampling occasions. Salinity and TDS showed broadly similar descriptive patterns, with lower values during the first neap occasion and higher values during later spring occasions, particularly Spring 2 and Spring 3. In contrast, pH varied within a narrower range and tended to be lower during the later spring occasions than during the earlier sampling occasions. These patterns indicate that surface-water conditions were not uniform during the dry-season survey period.

The similarity between salinity and TDS patterns is expected because both variables are related to dissolved ionic concentration in surface water. In mangrove and estuarine environments, salinity and TDS may vary over short temporal scales due to tidal exchange, freshwater input, evaporation, rainfall, and local hydrological connectivity. Salinity, flooding, and other physicochemical conditions are widely recognized as important environmental drivers of mangrove establishment and early development [68]. The descriptive PCA supported this relationship by showing that PC1 was positively associated with salinity and TDS and negatively associated with pH. This axis therefore represented a water-quality gradient from lower salinity/TDS and higher pH toward higher salinity/TDS and lower pH. However, because the number of independent sampling occasions was limited, this gradient is interpreted as a descriptive summary of the measured water-quality profiles rather than as evidence of a general tidal-period effect.

Plot-level variation within the same sampling occasion also indicates spatial heterogeneity within the replanted stand. Plots sampled on the same date shared the same broader temporal condition, but they still showed variation in water-quality values. This suggests that fine-scale conditions within the stand may influence local water properties. Possible factors include differences in plot elevation, proximity to tidal channels, water residence time, shading, sediment texture, and small-scale hydrological connectivity. Hydrology and local site conditions are central considerations in mangrove rehabilitation and restoration, particularly because unsuitable hydrological or substrate conditions may limit mangrove establishment and development [15]. However, these mechanisms were not tested directly in this study.

Sediment texture differed descriptively among transects and provided additional physical context for interpreting the replanted stand. Transect 1 was dominated by sand, which accounted for 60% of the sediment composition, followed by clay at 25% and silt at 15%. In contrast, Transects 2 and 3 were dominated by finer sediment fractions, particularly clay, which accounted for 54% and 59% of sediment composition, respectively. Sand content decreased from Transect 1 to Transect 3, while clay content increased across the same transect sequence. This pattern indicates that the physical substrate was not uniform across the replanted stand, with Transect 1 representing a sandier substrate and Transects 2 and 3 representing finer, more clay-rich substrates.

Sediment texture may be relevant to both vegetation structure and surface-active brachyuran assemblages. In mangrove habitats, sediment texture can influence drainage, water retention, sediment stability, root anchorage, propagule establishment, crab burrowing, and sediment reworking [15,16,68]. Finer sediments may retain more water and organic material, whereas sandier sediments may drain more rapidly and provide different microhabitat conditions. However, because sediment samples were composited at the transect level before laboratory analysis, the sediment data cannot be directly linked to plot-level vegetation or crab assemblage variation in the present study.

4.4. Present Condition of an Eight-Year-Old Replanted *Rhizophora mucronata* Stand

Taken together, the vegetation, sediment, surface-water, and brachyuran datasets characterize the present condition of the eight-year-old replanted *R. mucronata* stand at Sungai Ujung as taxonomically uniform in its living vegetation but structurally, physically, and biologically heterogeneous. The vegetation consisted entirely of *R. mucronata* and included an established tree layer and visible seedlings, but pole-stage individuals were sparsely represented. Sediment texture showed a descriptive transition from the relatively sandy substrate of Transect 1 to the finer, more clay-rich substrates of Transects 2 and 3. The selected surface-water physicochemical variables varied among the five dry-season sampling occasions and, to a lesser extent, among plots sampled on the same occasion. Meanwhile, the observed surface-active brachyuran assemblage was strongly uneven, with numerical dominance by *M. latifrons* and occasion- and plot-specific variation in abundance, taxonomic-unit richness, and diversity.

The observed heterogeneity should not, however, be interpreted automatically as either ecological improvement or degradation. It may reflect several overlapping influences, including the original planting configuration, survival of planted individuals, subsequent seedling recruitment and mortality, variation in surface elevation and tidal connectivity, sedimentary processes, transient surface-water conditions, and taxon-specific crab activity and detectability. The age of the plantation provides chronological context, but it does not identify a particular developmental stage or degree of recovery. An eight-year-old stand may contain established trees and associated fauna while still differing substantially from natural mangroves in vegetation composition, structural complexity, sediment properties, faunal assemblages, or ecosystem functioning. Restoration outcomes are known to vary with the ecosystem attribute measured, restoration method, stand age, and the reference condition used for comparison [57]. Accordingly, no single observation in the present study, including tree survival, seedling abundance, crab abundance, or the age of the stand, can serve independently as evidence of replantation success.

The combined results demonstrate the value of assessing planted mangroves through multiple habitat components. Vegetation measurements describe floristic composition and size structure but cannot alone establish whether appropriate physical conditions and faunal associations have developed. Sediment and surface-water measurements add information about the physical and physicochemical habitat template, whereas brachyuran observations provide a partial description of an ecologically important faunal component. This multidimensional perspective is consistent with proposed mangrove restoration-monitoring frameworks that incorporate project history, pre-restoration conditions, intervention characteristics, environmental setting, ecological outcomes, and socioeconomic dimensions [58,69]. A systematic review of 335 Southeast Asian mangrove restoration publications similarly found that research was concentrated on selected biodiversity attributes, particularly flora and fauna, while several ecosystem functions and social dimensions remained less frequently evaluated [70]. The present study addresses part of this imbalance by combining vegetation, sediment, surface-water, and faunal observations, although it does not measure ecosystem functions directly.

The eight-year-old replanted *R. mucronata* stand currently supports living *R. mucronata* trees, a spatially uneven seedling layer, a limited pole component, heterogeneous transect-scale sediment texture, temporally variable surface-water conditions, and a numerically uneven surface-active brachyuran assemblage dominated by *M. latifrons*. These attributes demonstrate the establishment of a planted mangrove habitat containing both vegetation and associated brachyuran fauna, but they do not demonstrate functional equivalence to a natural forest, successful self-replacement of the planted population, or recovery of ecosystem processes. Likewise, the numerical dominance of *M. latifrons* does not establish

functional recovery, and seedling presence does not establish successful recruitment into later growth stages.

Future studies should use permanent, spatially matched plots in which vegetation, sediment, surface and porewater conditions, hydrology, and brachyuran assemblages are measured at compatible spatial and temporal scales. Vegetation monitoring should quantify survival, growth, mortality, and transitions among size classes; sediment measurements should be replicated at plot level; and continuous water-level and salinity records should encompass multiple tidal cycles and seasons. Crab sampling should combine standardized surface observations with methods capable of detecting cryptic and burrow-retreating taxa. Including comparable natural and unrestored reference sites would provide the basis for evaluating direction and magnitude of change. With sufficient replication, hierarchical models could then test whether hydrology and sediment influence vegetation structure directly, whether vegetation mediates crab assemblage composition, and whether crab activity feeds back on sediment conditions. Until such data are available, the present study is best understood as an integrated baseline characterization from which these relationships and future trajectories can be tested.

5. Conclusions

This study provides a preliminary dry-season post-plantation habitat characterization of an eight-year-old replanted *R. mucronata* stand at Sungai Ujung River, South Sulawesi, Indonesia. The findings show that the site supports an established *R. mucronata* tree layer and visible seedling presence, but pole-stage individuals were scarce, indicating limited representation of intermediate stand structure. Sediment texture varied descriptively among transects, with a sand-dominated substrate in Transect 1 and finer, clay-dominated sediments in Transects 2 and 3.

The surface-active brachyuran assemblage comprised eight taxonomic units and was strongly dominated by *M. latifrons*. Crab abundance, Shannon diversity, and taxonomic-unit richness varied among sampling occasions and plots, indicating occasion-specific and within-site spatial heterogeneity. Selected surface-water variables also varied across the five valid sampling occasions, and the descriptive PCA summarized a gradient associated mainly with salinity, TDS, and pH. However, because tidal period was a sampling-occasion-level condition and only three spring-tide and two neap-tide occasions were available, these patterns should be interpreted descriptively rather than as evidence of general spring–neap tidal effects.

Overall, this study establishes a structured reference point for future monitoring of the Sungai Ujung replanted mangrove area. Because no pre-plantation baseline, long-term monitoring record, natural reference site, or unrestored control site was available, these findings should not be interpreted as evidence of replantation success, recovery trajectory, or functional recovery. Future studies should include repeated wet- and dry-season sampling, greater temporal replication across tidal conditions, plot-level sediment analysis, more comprehensive crab sampling methods, and comparison with reference and degraded mangrove sites to evaluate stand development and ecosystem functioning more rigorously.

Author Contributions: Conceptualization, A.F., M.K. and I.A.; Methodology, A.F.; Software, A.F.; Validation, A.F., I.A., M.K. and A.D.; Formal Analysis, A.F.; Investigation, A.F.; Resources, A.F.; Data Curation, A.F.; Writing—Original Draft Preparation, A.F.; Writing—Review and Editing, A.F., I.A., M.K., A.D. and R.I.M.; Visualization, A.F.; Supervision, I.A. and M.K.; Project Administration, I.A.; Funding Acquisition, I.A., A.D. and M.K. All authors have read and agreed to the published version of the manuscript.

Funding: This research was funded by Institut Teknologi Bandung Ganesha Talent Assistantship-Research Group (GTA-RG) 100 grant number 498/IT1.A/ SK-KM/2021 (PPMI-2021- awarded to IA) and Vrije Universiteit Brussel Universitas Call grant 2023. Part of this research is also funded by the Indonesian Endowment Fund for Education (LPDP) on behalf of the Indonesian Ministry of Higher Education, Science and Technology and managed under the EQUITY Program (Contract No. 4298/B3/DT.03.08/2025—awarded to AD).

Data Availability Statement: The nucleotide sequences generated in the study are openly available in GenBank under accession numbers PZ509682, PZ476711, PZ476807, PZ476801, PZ476748, PZ476808, PZ480361, PZ476802, and PZ476810.

Acknowledgments: The authors sincerely thank Bapak Burhan and Ibu Yupa for their assistance with field sampling and logistical support during the study. We are also grateful to Wa Ode Ainayah, Angel Patricia Komaling, Wulandari, Nuramaliah Jabbar, Awaluddin, Agung Dewa Putra, Akhyar Hamdi, and Aldin Al Rasyid Laora for their valuable assistance during sample collection. We thank Kushlani Disyanake and Timothy Sierens for technical support during the PCR analyses. Finally, the authors appreciate the constructive comments and suggestions provided by the reviewers, which helped improve the quality and clarity of this manuscript. The authors have reviewed and edited the output and take full responsibility for the content of this publication.

Conflicts of Interest: The authors declare no conflicts of interest.

Abbreviations

The following abbreviations are used in this manuscript:

DBH Diameter at Breast Height
PCR Polymerase Chain Reaction

Appendix A

Table A1. GenBank accession information for COI sequences generated in this study, including accession number, specimen code, morphotype, transect of origin, collection data, sequence length, final taxonomic assignment, and voucher information. (*) Sequences are deposited in GenBank but were not used for final molecular taxonomic validation because no suitable BOLD match was recovered, the closest GenBank matches showed low similarity, and phylogenetic placement was unstable.

Accession Number	Morphotype's Specimen Code	Morphotype	Transect	Collection Date	Sequence Length (Base Pair, bp)	Final Taxonomic Assignment	Voucher Information
PZ509682 *	B3	Sesarmidae	2	16 August 2023	560	Sesarmidae	WSIC2
PZ476711	C1	Parasesarma	1	16 August 2023	588	Parasesarma	WSIC1
PZ476807	C3a	Parasesarma	2	16 August 2023	585	Parasesarma	WSIC9
PZ476801 *	F3	Gecarcinidae	3	24 August 2023	585	Gecarcinidae	WSIC8
PZ476748	G1	*Metaplax elegans*	1	18 July 2023	585	*Metaplax elegans*	WSIC3
PZ476808	G2	*Metaplax elegans*	2	18 July 2023	591	*Metaplax elegans*	WSIC4
PZ480361	G3	*Metaplax elegans*	3	18 July 2023	597	*Metaplax elegans*	WSIC5
PZ476802	H1	*Metopograpsus latifrons*	1	18 July 2023	588	*Metopograpsus latifrons*	WSIC7
PZ476810	H2	*Metopograpsus latifrons*	2	18 July 2023	597	*Metopograpsus latifrons*	WSIC6

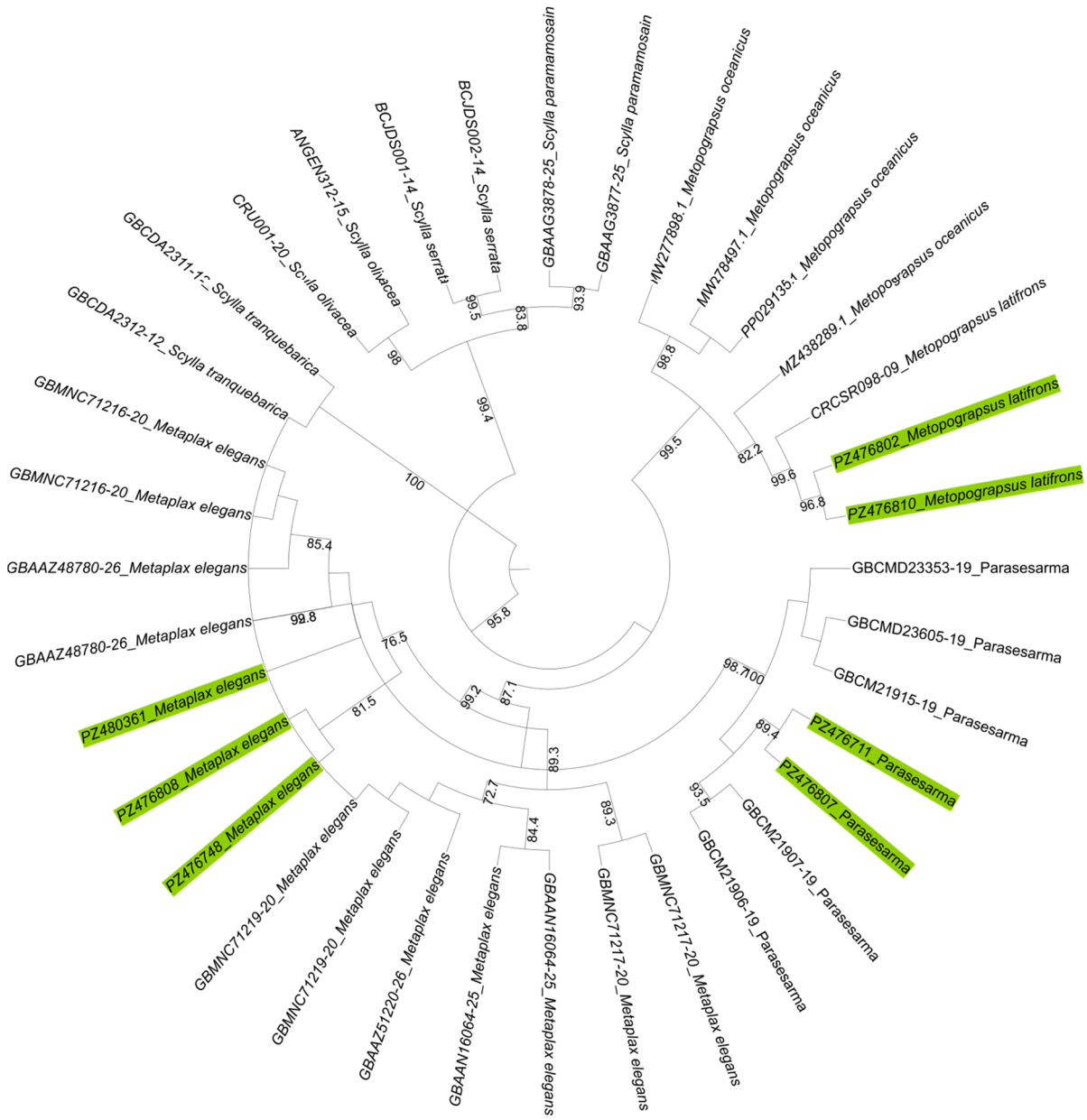


Figure A1. Maximum-likelihood phylogenetic tree based on a 627-column aligned COI matrix containing eight accepted study sequences and 29 reference or outgroup sequences. Study sequences ranged from 560 to 597 bp, and missing terminal positions in shorter sequences were represented as terminal gaps and treated as missing data. Node support was assessed using 1000 bootstrap replicates, and only bootstrap values ≥ 70 are shown. Sequences generated in this study are blocked in green. Sequences of *Scylla olivacea*, *S. tranquebarica*, *S. paramamosain*, and *S. serrata* were included as outgroups to root the phylogeny.

Table A2. Reference sequences and taxonomic assignments used to validate the identity of surface-active taxonomic units collected at Sungai Ujung River, South Sulawesi, Indonesia. Taxonomic assignments were based on morphological identification, DNA barcoding, sequence similarity searches in BOLD and GenBank, and phylogenetic clustering in the maximum-likelihood COI tree. Shaded cells indicate unavailable or non-applicable data for the corresponding morphotype and reference source.

Morphotype	Final Assignment on Taxonomic Unit	Gen Bank Accession Number	Top BOLD Match (Taxonomic Assignment)	BOLD Processing ID (PID) and Barcode Index Number (BIN)	Top GenBank Match (Taxonomic Assignment)	Reference Genbank Accession Number	Percent Identity	Query Coverage	Alignment Score	Number of Unclear Base	Phylogenetic Node Support
B	Sesarmidae	PZ509682 (Not used for validation)			*Sesarma schubarti*	PP431261.1	89.5	99	0	27	Low percent identity with references
					Sesarma rhizophorae	OQ396661.1	89.6	96	0		
					Sinosesarma tangi	LC500793.1	89.42	96	0		
					Sesarma sp.	PV781382.1	89.42	96	0		
					Chiromantes haematocheir	MT017656.1	89.01	98	0		
					Sesarma rubinofforum	OQ396665.1	89.6	96	0		
					Sesarma reticulatum	KX400927.1	89.93	94	0		
					Sesarma curacaoense	MN183990.1	89.05	96	0		
					Sesarma curacaoense	MN184196.1	89.05	96	0		
					Sesarma curacaoense	MN183914.1	89.05	96	0		
C	Parasesarma	PZ476711	Parasesarma	GBCM21915-19 [BOLD:AEB6586]			99.45			0	89.4
			Parasesarma messa	GBCMD23353-19 [BOLD:AEB6586]			99.4				
			Parasesarma messa	GBCMD23605-19 [BOLD:AEB6586]			99.45				
			Parasesarma	GBCM21906-19 [BOLD:AEB6586]			98.90				
			Parasesarma	GBCM21907-19 [BOLD:AEB6586]			99.08				
C	Parasesarma	PZ476807	Parasesarma	GBCM21915-19 [BOLD:AEB6586]			99.45			0	89.4
			Parasesarma messa	GBCMD23353-19 [BOLD:AEB6586]			99.4				
			Parasesarma messa	GBCMD23605-19 [BOLD:AEB6586]			99.45				
			Parasesarma	GBCM21906-19 [BOLD:AEB6586]			98.90				
			Parasesarma	GBCM21907-19 [BOLD:AEB6586]			99.08				

Table A2. *Cont.*

Morphotype	Final Assignment on Taxonomic Unit	Gen Bank Accession Number	Top BOLD Match (Taxonomic Assignment)	BOLD Processing ID (PID) and Barcode Index Number (BIN)	Top GenBank Match (Taxonomic Assignment)	Reference Genbank Accession Number	Percent Identity	Query Coverage	Alignment Score	Number of Unclear Base	Phylogenetic Node Support
F	Gecarcinidae	PZ476801 (Not used for validation)			*Gecarcoidea lalandii*	LC225573.1	86.76	98	0	0	Unstable phylogenetic placement; sequence not used for final molecular taxonomic validation
					Grimothea gregaria	KU728417.1	86.5	100	0		
					Metaplax elegans	PV640763.1	86.97	97	0		
					Metaplax elegans	LC498182.1	86.97	97	0		
					Gecarcoidea lalandii	LC225581.1	86.76	98	0		
G	*Metaplax elegans*	PZ476748	*Metaplax elegans*	GBMNC71216-20 [BOLD:ADQ9400]			100			0	81.5
			Metaplax elegans	GBAAZ48780-26 [BOLD:ADQ9400]			99.76				
			Metaplax elegans	GBMNC71217-20 [BOLD:ADQ9400]			99.60				
			Metaplax elegans	GBMNC71219-20 [BOLD:ADQ9400]			99.52				
			Metaplax elegans	GBAAN16064-25 [BOLD:ADQ9400]			98.45				
G	*Metaplax elegans*	PZ476808	*Metaplax elegans*	GBMNC71216-20 [BOLD:ADQ9400]			100			0	81.5
			Metaplax elegans	GBAAZ48780-26 [BOLD:ADQ9400]			99.76				
			Metaplax elegans	GBMNC71219-20 [BOLD:ADQ9400]			99.60				
			Metaplax elegans	GBAAN16064-25 [BOLD:ADQ9400]			99.52				
			Metaplax elegans	GBAAZ51220-26 [BOLD:ADQ9400]			98.45				
G	*Metaplax elegans*	PZ480361	*Metaplax elegans*	GBMNC71216-20 [BOLD:ADQ9400]			100			0	76.5
			Metaplax elegans	GBAAZ48780-26 [BOLD:ADQ9400]			99.76				
			Metaplax elegans	GBMNC71217-20 [BOLD:ADQ9400]			99.60				
			Metaplax elegans	GBMNC71219-20 [BOLD:ADQ9400]			99.52				
			Metaplax elegans	GBAAN16064-25 [BOLD:ADQ9400]			98.45				

Table A2. *Cont.*

Morphotype	Final Assignment on Taxonomic Unit	Gen Bank Accession Number	Top BOLD Match (Taxonomic Assignment)	BOLD Processing ID (PID) and Barcode Index Number (BIN)	Top GenBank Match (Taxonomic Assignment)	Reference Genbank Accession Number	Percent Identity	Query Coverage	Alignment Score	Number of Unclear Base	Phylogenetic Node Support
H	*Metopograpsus latifrons*	PZ476802	*Metopograpsus latifrons*	CRCSR098-09 [BOLD:AAF9321]			99.40			0	96.8
					Metopograpsus oceanicus	PP029135.1	99.99	100	0		
					Metopograpsus oceanicus	MW278497.1	99.99	100	0		
					Metopograpsus oceanicus	MW277898.1	99.80	100	0		
					Metopograpsus sp.	MZ438289.1	99.80	90	0		
H	*Metopograpsus latifrons*	PZ476810	*Metopograpsus latifrons*	CRCSR098-09 [BOLD:AAF9321]			99.40			0	96.8
					Metopograpsus oceanicus	PP029135.1	99.99	100	0		
					Metopograpsus oceanicus	MW278497.1	99.99	100	0		
					Metopograpsus oceanicus	MW277898.1	99.80	100	0		
					Metopograpsus sp.	MZ438289.1	99.80	90	0		

Table A3. Outgroup sequences of *Scylla* spp. retrieved from the Barcode of Life Data System (BOLD) and included in the maximum-likelihood COI phylogenetic tree.

Species	BOLD Process ID
Scylla olivacea	ANGEN312-15
S. olivacea	CRU001-20
S. tranquebarica	GBCDA2311-12
S. tranquebarica	GBCDA2312-12
S. paramamosain	GBAAG3877-25
S. paramamosain	GBAAG3878-25
S. serrata	BCJDS002-14
S. serrata	BCJDS001-14

Table A4. Full-survey descriptive summary of surface-active brachyuran taxonomic units. Single asterisk (*) indicates identification supported by morphological characteristics and DNA barcoding; double asterisk (**) indicates morphology-based identification retained because molecular validation was unavailable or unsuitable.

Morphotype	Final Assignment of Taxonomic Unit	Total Abundance	Relative Abundance (%)	Occurrence Plot-Occasions	Plots Detected	Occasions Detected
H	*Metopograpsus latifrons* (White, 1847) *	414	61.2	30	7	5
F	Gecarcinidae MacLeay, 1838 **	82	12.1	10	7	3
G	*Metaplax elegans* De Man, 1888 *	56	8.28	9	6	4
C	*Parasesarma* De Man, 1895 *	47	6.95	5	3	3
E	Ocypodidae Rafinesque, 1815 2 **	36	5.32	3	2	2
A	Sesarmidae Dana, 1851 1 **	23	3.40	4	4	2
B	Sesarmidae Dana, 1851 2 **	10	1.48	3	3	2
D	Ocypodidae Rafinesque, 1815 1 **	8	1.18	3	3	3

Table A5. Overall descriptive summary of selected surface-water variables. Values represent plot × sampling occasion observations across five valid sampling occasions. Q1 = first quartile; Q3 = third quartile; IQR = interquartile range; SD = standard deviation; TDS = total dissolved solids.

Variable	Unit	*n* Observations	*n* Plots	*n* Sampling Occasions	Median	Q1	Q3	IQR	Min	Max	Mean	SD
Salinity	-	35	7	5	15	12	22.5	10.5	8	27	16.6	5.66
TDS	ppm	35	7	5	5480	4560	6755	2195	1900	9180	5808	1911
pH	-	35	7	5	6.9	6.7	7.3	0.6	6.5	8.2	7.03	0.367

References

1. Bimrah, K.; Dasgupta, R.; Hashimoto, S.; Saizen, I.; Dhyani, S. Ecosystem Services of Mangroves: A Systematic Review and Synthesis of Contemporary Scientific Literature. *Sustainability* **2022**, *14*, 12051. [CrossRef]
2. Akram, H.; Hussain, S.; Mazumdar, P.; Chua, K.O.; Butt, T.E.; Harikrishna, J.A. Mangrove Health: A Review of Functions, Threats, and Challenges Associated with Mangrove Management Practices. *Forests* **2023**, *14*, 1698. [CrossRef]
3. Owuor, M.; Santos, T.M.T.; Otieno, P.; Mazzuco, A.C.A.; Iheaturu, C.; Bernardino, A.F. Flow of Mangrove Ecosystem Services to Coastal Communities in the Brazilian Amazon. *Front. Environ. Sci.* **2024**, *12*, 1329006. [CrossRef]
4. Alongi, D.M. Global Meta-Analysis of Mangrove Primary Production: Implications for Carbon Cycling in Mangrove and Other Coastal Ecosystems. *Forests* **2025**, *16*, 747. [CrossRef]
5. Bosire, J.O.; Dahdouh-Guebas, F.; Walton, M.; Crona, B.I.; Lewis, R.R.; Field, C.; Kairo, J.G.; Koedam, N. Functionality of Restored Mangroves: A Review. *Aquat. Bot.* **2008**, *89*, 251–259. [CrossRef]
6. Ilman, M.; Wibisono, I.T.C.; Suryadiputra, I.N.N. *State of the Art Information on Mangrove Ecosystems in Indonesia*; Wetlands International-Indonesia Programme: Bogor, Indonesia, 2011.
7. Ilman, M.; Dargusch, P.; Dart, P.; Onrizal. A Historical Analysis of the Drivers of Loss and Degradation of Indonesia's Mangroves. *Land Use Policy* **2016**, *54*, 448–459. [CrossRef]
8. Dahdouh-Guebas, F.; Cannicci, S. Mangrove Restoration Under Shifted Baselines and Future Uncertainty. *Front. Mar. Sci.* **2021**, *8*, 799543. [CrossRef]
9. Djamaluddin, R.; Fusi, M.; Djabar, B.; Evans, D.; Holmes, R.; Huxham, M.; O'Connell, D.P.; Salzmann, U.; Singleton, I.; Tjoa, A.; et al. Point of (No) Return? Vegetation Structure and Diversity of Restored Mangroves in Sulawesi, Indonesia, 14–16 Years On. *Restor. Ecol.* **2023**, *31*, e13963. [CrossRef]
10. Sasmito, S.D.; Basyuni, M.; Kridalaksana, A.; Saragi-Sasmito, M.F.; Lovelock, C.E.; Murdiyarso, D. Challenges and Opportunities for Achieving Sustainable Development Goals through Restoration of Indonesia's Mangroves. *Nat. Ecol. Evol.* **2023**, *7*, 62–70. [CrossRef] [PubMed]
11. Menteri Kehutanan Republik Indonesia. *Keputusan Menteri Kehutanan Republik Indonesia Nomor 594 Tahun 2024 Tentang Peta Mangrove Nasional Tahun 2024*; Kementerian Kehutanan Republik Indonesia: Jakarta, Indonesia, 2024.
12. Kauffman, J.B.; Donato, D.C. *Protocols for the Measurement, Monitoring and Reporting of Structure, Biomass and Carbon Stocks in Mangrove Forests. Working Paper 86*; Center for International Forestry Research (CIFOR): Bogor, Indoensia, 2012.
13. Cannicci, S.; Lee, S.Y.; Bravo, H.; Cantera-Kintz, J.R.; Dahdouh-Guebas, F.; Fratini, S.; Fusi, M.; Jimenez, P.J.; Nordhaus, I.; Porri, F.; et al. A Functional Analysis Reveals Extremely Low Redundancy in Global Mangrove Invertebrate Fauna. *Proc. Natl. Acad. Sci. USA* **2021**, *118*, e2016913118. [CrossRef] [PubMed]
14. Nordhaus, I.; Hadipudjana, F.A.; Janssen, R.; Pamungkas, J. Spatio-Temporal Variation of Macrobenthic Communities in the Mangrove-Fringed Segara Anakan Lagoon, Indonesia, Affected by Anthropogenic Activities. *Reg. Environ. Change* **2009**, *9*, 291–313. [CrossRef]
15. Aschenbroich, A.; Michaud, E.; Stieglitz, T.; Fromard, F.; Gardel, A.; Tavares, M.; Thouzeau, G. Brachyuran Crab Community Structure and Associated Sediment Reworking Activities in Pioneer and Young Mangroves of French Guiana, South America. *Estuar. Coast. Shelf Sci.* **2016**, *182*, 60–71. [CrossRef]
16. Kristensen, E. Mangrove Crabs as Ecosystem Engineers; with Emphasis on Sediment Processes. *J. Sea Res.* **2008**, *59*, 30–43. [CrossRef]
17. Neely, S.H. Effects of Bioturbation by the Fiddler Crab *Leptuca Speciosa* (Ives, 1891) (Decapoda: Brachyura: Ocypodidae) on Mangrove Peat in Barnes Sound, Florida, USA. *J. Crustac. Biol.* **2023**, *43*, ruad006. [CrossRef]
18. Bellwood, O. The Occurrence, Mechanics and Significance of Burying Behaviour in Crabs (Crustacea: Brachyura). *J. Nat. Hist.* **2002**, *36*, 1223–1238. [CrossRef]
19. Amalo, L.F.; Putra, M.D.; Handayani, L.D.W.; Sumpeno, S.; Luturmas, R.; Suryadi, S. The Determination of Mangrove Restoration Area Using Water Quality and Substrate Parameters. *Medkon* **2025**, *30*, 84. [CrossRef]
20. Das, L.; Patel, R.; Salvi, H.; Kamboj, R.D. Assessment of Natural Regeneration of Mangrove with Reference to Edaphic Factors and Water in Southern Gulf of Kachchh, Gujarat, India. *Heliyon* **2019**, *5*, e02250. [CrossRef] [PubMed]
21. Walton, M.E.; Le Vay, L.; Lebata, J.H.; Binas, J.; Primavera, J.H. Assessment of the Effectiveness of Mangrove Rehabilitation Using Exploited and Non-Exploited Indicator Species. *Biol. Conserv.* **2007**, *138*, 180–188. [CrossRef]
22. Basyuni, M.; Gultom, K.; Fitri, A.; Susetya, I.E.; Wati, R.; Slamet, B.; Sulistiyono, N.; Yusriani, E.; Balke, T.; Bunting, P. Diversity and Habitat Characteristics of Macrozoobenthos in the Mangrove Forest of Lubuk Kertang Village, North Sumatra, Indonesia. *Biodiversitas* **2018**, *19*, 311–317. [CrossRef]
23. Ocaña, F.A.; De Jesús-Navarrete, A. Using Indirect Methods to Estimate Population Parameters of the Atlantic Ghost Crab from Beaches in Northeastern Cuba. *Reg. Stud. Mar. Sci.* **2021**, *43*, 101705. [CrossRef]
24. Patel, K.; Patel, H.; Ali, D.; Gosavi, S.; Choudhary, N.; Yadav, V.K.; Vachhrajani, K.; Patel, A.; Sahoo, D.K.; Trivedi, J. On Population Structure and Breeding Biology of Burrowing Crab *Dotilla blanfordi* Alcock, 1900. *PeerJ* **2024**, *12*, e17065. [CrossRef] [PubMed]

25. Ashton, E.C.; Macintosh, D.J. Mangrove Rehabilitation and Brachyuran Crab Biodiversity in Ranong, Thailand. *Diversity* **2024**, *16*, 92. [CrossRef]
26. Rahim, H.A.; Shuhaida, S.; Yahya, K. Rapid Baseline Assessment of Crab Abundance and Species Richness in Mangroves Using a Video Recording Method. *IOP Conf. Ser. Earth Environ. Sci.* **2021**, *736*, 012056. [CrossRef]
27. Ngo-Massou, V.; Essome-Koum, G.; Ngollo-Dina, E.; Din, N. Composition of Macrobenthos in the Wouri River Estuary Mangrove, Douala, Cameroon. *Afr. J. Mar. Sci.* **2012**, *34*, 349–360. [CrossRef]
28. Gordon, I. Brachyura from the Coasts of China. *J. Linn. Soc. Lond. Zool.* **1931**, *37*, 525–558. [CrossRef]
29. Tweedie, M.W.F. The Species of Metopograpsus (Crustacea, Brachyura). *Bijdr. Dierkd.* **1949**, *28*, 466–471. [CrossRef]
30. Campbell, B.M. The Australian Sesarminae (Crustacea: Brachyura): Five Species of Sesarma (Chiromanthes). *Mem. Qld. Mus. Nat.* **1967**, *15*, 1–19.
31. Serene, R.; Soh, C.L. Note on the Five Largest Species of Sesarma Crabs in Malaysia and Singapore. *Malay. Nat. J.* **1967**, *20*, 27–30.
32. Serene, R.; Soh, C.L. New Indo-Pacific Genera Allied to Sesarma Say, 1817 (Brachyura, Decapoda, Crustacea). *Treubia* **1970**, *27*, 387–417.
33. Gillikin, D.P.; Schubart, C.D. Ecology and Systematics of Mangrove Crabs of the Genus Perisesarma (Crustacea: Brachyura: Sesarmidae) from East Africa. *Zool. J. Linn. Soc.* **2004**, *141*, 435–445. [CrossRef]
34. Ng, P.K.L.; Guinot, D.; Davie, P.J.F. Systema Brachyurorum: Part I. An Annotated Checklist of Extant Brachyuran Crabs of the World. *Raffles Bull. Zool.* **2008**, *17*, 1–286.
35. Weineck, K.; Ray, A.J.; Fleckenstein, L.J.; Medley, M.; Dzubuk, N.; Piana, E.; Cooper, R.L. Physiological Changes as a Measure of Crustacean Welfare under Different Standardized Stunning Techniques: Cooling and Electroshock. *Animals* **2018**, *8*, 158. [CrossRef] [PubMed]
36. Rumisha, C.; Huyghe, F.; Rapanoel, D.; Mascaux, N.; Kochzius, M. Genetic Diversity and Connectivity in the East African Giant Mud Crab Scylla Serrata: Implications for Fisheries Management. *PLoS ONE* **2017**, *12*, e0186817. [CrossRef] [PubMed]
37. Folmer, O.; Black, M.; Hoeh, W.; Lutz, R.; Vrijenhoek, R. DNA Primers for Amplification of Mitochondrial Cytochrome c Oxidase Subunit I from Diverse Metazoan Invertebrates. *Mol. Mar. Biol. Biotechnol.* **1994**, *3*, 294–299. [PubMed]
38. Kettler, T.A.; Doran, J.W.; Gilbert, T.L. Simplified Method for Soil Particle-Size Determination to Accompany Soil-Quality Analyses. *Soil Sci. Soc. Am. J.* **2001**, *65*, 849–852. [CrossRef]
39. Dahdouh-Guebas, F. World Mangroves Database. Available online: https://www.marinespecies.org/mangroves (accessed on 30 July 2025).
40. Katoh, K.; Standley, D.M. MAFFT Multiple Sequence Alignment Software Version 7: Improvements in Performance and Usability. *Mol. Biol. Evol.* **2013**, *30*, 772–780. [CrossRef] [PubMed]
41. Wong, T.K.F.; Ly-Trong, N.; Ren, H.; Demotte, P.; Baños, H.; Roger, A.J.; Susko, E.; Bielow, C.; De Maio, N.; Goldman, N.; et al. IQ-TREE 3: Phylogenomic Inference Software Using Complex Evolutionary Models. *Mol. Biol. Evol.* **2026**, *43*, msag117. [CrossRef] [PubMed]
42. Letunic, I.; Bork, P. Interactive Tree of Life (iTOL) v6: Recent Updates to the Phylogenetic Tree Display and Annotation Tool. *Nucleic Acids Res.* **2024**, *52*, W78–W82. [CrossRef] [PubMed]
43. Spellerberg, I.F. Shannon–Wiener Index. In *Encyclopedia of Ecology*; Elsevier: Amsterdam, The Netherlands, 2008; pp. 3249–3252. ISBN 978-0-08-045405-4.
44. Snedaker, S.C.; Snedaker, J.G.; Working Group 60 On Mangrove Ecology (Eds.) The Mangrove Ecosystem: Research Methods. In *Monographs on Oceanographic Methodology*; UNESCO: Paris, France, 1984.
45. R Core Team. *R: A Language and Environment for Statistical Computing*; R Foundation for Statistical Computing: Vienna, Austria, 2026.
46. Wickham, H.; Bryan, J. *Readxl: Read Excel Files*, Version 1.5.0; Posit, PBC: Boston, MA, USA, 2015.
47. Wickham, H.; Averick, M.; Bryan, J.; Chang, W.; McGowan, L.D.; François, R.; Grolemund, G.; Hayes, A.; Henry, L.; Hester, J.; et al. Welcome to the tidyverse. *J. Open Source Softw.* **2019**, *4*, 1686. [CrossRef]
48. Wickham, H. *Ggplot2: Elegant Graphics for Data Analysis*, Use R! 2nd ed. Springer International Publishing: Cham, Switzerland, 2016.
49. Wickham, H.; François, R.; Henry, L.; Müller, K.; Vaughan, D. *Dplyr: A Grammar of Data Manipulation 2014*, Version 1.2.1; Posit, PBC: Boston, MA, USA, 2014.
50. Wickham, H.; Vaughan, D.; Girlich, M. *Tidyr: Tidy Messy Data*, Version 1.3.2.; Posit, PBC: Boston, MA, USA, 2014.
51. Wickham, H.; Henry, L. *Purrr: Functional Programming Tools*, Version 1.2.2.; Posit, PBC: Boston, MA, USA, 2016.
52. Müller, K.; Wickham, H. *Tibble: Simple Data Frames*, Version 3.3.1.; Posit, PBC: Boston, MA, USA, 2016.
53. Wickham, H. *Stringr: Simple, Consistent Wrappers for Common String Operations*, Version 1.6.0.; Posit, PBC: Boston, MA, USA, 2009.
54. Wickham, H. *Forcats: Tools for Working with Categorical Variables (Factors)*, Version 1.0.1.; Posit, PBC: Boston, MA, USA, 2016.
55. Amin, F.; Paransa, D.S.J.; Ompi, M.; Mantiri, D.H.M.; Boneka, F.B.; Kalesaran, O. Identifikasi Morfologi Dan Keanekaragaman Kepiting Pada Timbunan Berbatu Di Pantai Pesisir Malalayang Dua Kota Manado. *J. Pesisir Laut. Trop.* **2021**, *9*, 123–132. [CrossRef]

56. Paransa, D.S.J.; Kemer, K.; Kepel, R.C.; Mantiri, D.H.M.; Kolondam, B.J. Morphological and Molecular Identification of Metopograpsus Crab Caught from the Coast of Tambala Village, North Sulawesi, Indonesia. *Fish. Aquat. Sci.* **2024**, *27*, 411–420. [CrossRef]
57. Su, J.; Friess, D.A.; Gasparatos, A. A Meta-Analysis of the Ecological and Economic Outcomes of Mangrove Restoration. *Nat. Commun.* **2021**, *12*, 5050. [CrossRef] [PubMed]
58. Gatt, Y.M.; Andradi-Brown, D.A.; Ahmadia, G.N.; Martin, P.A.; Sutherland, W.J.; Spalding, M.D.; Donnison, A.; Worthington, T.A. Quantifying the Reporting, Coverage and Consistency of Key Indicators in Mangrove Restoration Projects. *Front. For. Glob. Change* **2022**, *5*, 720394. [CrossRef]
59. Vermeiren, P.; Sheaves, M. Modeling Intertidal Crab Distribution Patterns Using Photographic Mapping Among Tropical Australian Estuaries. *Estuaries Coasts* **2015**, *38*, 1545–1556. [CrossRef]
60. Nordhaus, I.; Diele, K.; Wolff, M. Activity Patterns, Feeding and Burrowing Behaviour of the Crab Ucides Cordatus (Ucididae) in a High Intertidal Mangrove Forest in North Brazil. *J. Exp. Mar. Biol. Ecol.* **2009**, *374*, 104–112. [CrossRef]
61. Egawa, R.; Sharma, S.; Nadaoka, K.; MacKenzie, R.A. Burrow Dynamics of Crabs in Subtropical Estuarine Mangrove Forest. *Estuar. Coast. Shelf Sci.* **2021**, *252*, 107244. [CrossRef]
62. Vermeiren, P.; Sheaves, M. Predictable Habitat Associations of Four Crab Species Across the Low Intertidal Landscape of a Tropical Estuary over Time. *Estuaries Coasts* **2015**, *38*, 285–295. [CrossRef]
63. Ferreira, A.C.; Alencar, C.E.R.D.; Bezerra, L.E.A. Interrelationships among Ecological Factors of Brachyuran Crabs, Trees and Soil in Mangrove Community Assemblage in Northeast Brazil. *Community Ecol.* **2019**, *20*, 277–290. [CrossRef]
64. Ashton, E.C.; Hogarth, P.J.; Macintosh, D.J. A Comparison of Brachyuran Crab Community Structure at Four Mangrove Locations under Different Management Systems along the Melaka Straits-Andaman Sea Coast of Malaysia and Thailand. *Estuaries* **2003**, *26*, 1461–1471. [CrossRef]
65. Barnuevo, A.; Asaeda, T.; Sanjaya, K.; Kanesaka, Y.; Fortes, M. Drawbacks of Mangrove Rehabilitation Schemes: Lessons Learned from the Large-Scale Mangrove Plantations. *Estuar. Coast. Shelf Sci.* **2017**, *198*, 432–437. [CrossRef]
66. Djamaluddin, R.; Kaumbo, M.A.; Djabar, B. PRESENT CONDITION OF MANGROVE ENVIRONMENT AND COMMUNITY STRUCTURE IN TOMINI GULF, SULAWESI, INDONESIA. *J. Ilmu Teknol. Kelaut. Trop.* **2019**, *11*, 601–614. [CrossRef]
67. Sloey, T.M.; Lim, K.E.; Moore, J.; Heng, J.M.; Heng, J.M.; Van Breugel, M. Influence of Abiotic Drivers on 1-year Seedling Survival of Six Mangrove Species in Southeast Asia. *Restor. Ecol.* **2022**, *30*, e13694. [CrossRef]
68. Krauss, K.W.; Lovelock, C.E.; McKee, K.L.; López-Hoffman, L.; Ewe, S.M.L.; Sousa, W.P. Environmental Drivers in Mangrove Establishment and Early Development: A Review. *Aquat. Bot.* **2008**, *89*, 105–127. [CrossRef]
69. Gatt, Y.M.; Walton, R.W.; Andradi-Brown, D.A.; Spalding, M.D.; Acosta-Velázquez, J.; Adame, M.F.; Barros, F.; Beeston, M.A.; Bernardino, A.F.; Buelow, C.A.; et al. The Mangrove Restoration Tracker Tool: Meeting Local Practitioner Needs and Tracking Progress toward Global Targets. *One Earth* **2024**, *7*, 2072–2085. [CrossRef]
70. Gerona-Daga, M.E.B.; Salmo, S.G. A Systematic Review of Mangrove Restoration Studies in Southeast Asia: Challenges and Opportunities for the United Nation's Decade on Ecosystem Restoration. *Front. Mar. Sci.* **2022**, *9*, 987737. [CrossRef]

Disclaimer/Publisher's Note: The statements, opinions and data contained in all publications are solely those of the individual author(s) and contributor(s) and not of MDPI and/or the editor(s). MDPI and/or the editor(s) disclaim responsibility for any injury to people or property resulting from any ideas, methods, instructions or products referred to in the content.